

UNIVERSIDAD SAN FRANCISCO DE QUITO USFQ

Colegio de Posgrados

**Develop a Circuit Model to Forecast the Conducted
Electromagnetic Interference (EMI)**

Mecanismo de Titulación:

**Tesis en torno a una hipótesis o problema de investigación y su
contrastación**

Mr. Yandry Alexander Jácome Montero

**Dr. Adam Quotb
Director de Trabajo de Titulación**

Trabajo de titulación de posgrado presentado como requisito
para la obtención del título de Magíster en Nanoelectrónica, Mención en Sistema Embebido
e Integración

Quito, 10/02/2025

UNIVERSIDAD SAN FRANCISCO DE QUITO USFQ
COLEGIO DE POSGRADOS

HOJA DE APROBACIÓN DE TRABAJO DE TITULACIÓN

**Desarrollo de un modelo de circuito para predecir la interferencia
electromagnética conducida (EMI)**

Yandry Alexander Jacome Montero

Nombre del Director del Programa: Luis Miguel Prócel
Título académico: Doctor of Philosophy
Director del programa de: Maestría en Nanoelectrónica

Nombre del Decano del colegio Académico: Eduardo Alba
Título académico: Doctor of Philosophy
Decano del Colegio: Colegio de Ciencias e Ingenierías

Nombre del Decano del Colegio de Posgrados: Dario Niebieskikwiat
Título académico: Doctor of Physics

Quito, Febrero 2025

© DERECHOS DE AUTOR

Por medio del presente documento certifico que he leído todas las Políticas y Manuales de la Universidad San Francisco de Quito USFQ, incluyendo la Política de Propiedad Intelectual USFQ, y estoy de acuerdo con su contenido, por lo que los derechos de propiedad intelectual del presente trabajo quedan sujetos a lo dispuesto en esas Políticas.

Asimismo, autorizo a la USFQ para que realice la digitalización y publicación de este trabajo en el repositorio virtual, de conformidad a lo dispuesto en la Ley Orgánica de Educación Superior del Ecuador.

Nombre del estudiante: Yandry Alexander Jacome Monterol

Código de estudiante: 00331365

C.I.: 02024755051

Lugar y fecha: Quito, 10 de Febrero.

ACLARACIÓN PARA PUBLICACIÓN

Nota: El presente trabajo, en su totalidad o cualquiera de sus partes, no debe ser considerado como una publicación, incluso a pesar de estar disponible sin restricciones a través de un repositorio institucional. Esta declaración se alinea con las prácticas y recomendaciones presentadas por el Committee on Publication Ethics (COPE) descritas por Barbour et al. (2017) *Discussion document on best practice for issues around theses publishing*, disponible en <http://bit.ly/COPETheses>.

UNPUBLISHED DOCUMENT

Note: The following graduation project is available through Universidad San Francisco de Quito (USFQ) institutional repository. Nonetheless, this project – in whole or in part – should not be considered a publication. This statement follows the recommendations presented by the Committee on Publication Ethics (COPE) described by Barbour et al. (2017) *Discussion document on best practice for issues around theses publishing* available on <http://bit.ly/COPETheses>.

DEDICATION

Este trabajo está dedicado a mi familia, cuyo apoyo incondicional y guía han sido fundamentales en cada etapa de mi formación académica y profesional. A mis mentores y profesores, quienes con su conocimiento y orientación han enriquecido mi camino y fomentado mi pasión por la investigación. También, a mis colegas y amigos que han sido una fuente constante de motivación y aprendizaje. Finalmente, dedico este esfuerzo a todos aquellos que buscan superar los límites del conocimiento y la innovación en el campo de la ingeniería electrónica.

This work is dedicated to my family, whose unconditional support and guidance have been fundamental at every stage of my academic and professional journey. To my mentors and professors, whose knowledge and guidance have enriched my path and nurtured my passion for research. Also, to my colleagues and friends, who have been a constant source of motivation and learning. Finally, I dedicate this effort to all those who strive to push the boundaries of knowledge and innovation in the field of electronic engineering.

ACKNOWLEDGMENTS

I would like to express my sincere gratitude to everyone who made this project possible. In particular, to Dr. Mohamed TOURE, my supervisor, for his valuable guidance and continuous support. I also extend my thanks to Alexis DELEPIERRE, Alice FERREIRA, Julien MASSON, Marc BOUIX, Jawaher VERMERSCH, Damien CHANAVAT, Nina LORHO, Rene DUBOIS, and Dylan RIGAULT for their invaluable assistance and collaboration throughout the process. To all of them, as well as to many others who have been part of this experience, I am grateful for their commitment, patience, and for sharing their knowledge and time with me.

RESUMEN

Este proyecto presenta una metodología integral para la estimación de la interferencia electromagnética conducida (EMI) en fuentes de alimentación conmutadas (SMPS). El enfoque principal radica en el desarrollo de un modelo de circuito que predice las perturbaciones conducidas mediante simulaciones en los dominios del tiempo y la frecuencia. El estudio emplea el software LTspice para modelar una topología de fuente de alimentación compuesta por un convertidor de alta tensión operando en modo de conducción discontinua (DCM) y un convertidor de baja tensión operando en modo de conducción continua (CCM).

Además, el proyecto abarca los procesos de automatización y optimización de convertidores Buck en tres configuraciones: baja tensión, alta tensión y convertidores Buck dobles. Estos procesos fueron fundamentales para agilizar la evaluación de su rendimiento en términos de EMI, permitiendo ajustes rápidos de parámetros y logrando diseños óptimos. A través de una combinación de enfoques de simulación directa e indirecta, la investigación compara la precisión y eficiencia computacional de estos métodos con los resultados experimentales obtenidos mediante el dispositivo EMSCOPE. Los hallazgos demuestran la validez del modelado en el dominio de la frecuencia para la optimización de filtros de compatibilidad electromagnética (EMC), reduciendo la necesidad de pruebas iterativas de prototipos. Los resultados indican que la metodología propuesta puede anticipar eficazmente las perturbaciones conducidas, permitiendo así un diseño más temprano y eficiente de filtros EMC.

ABSTRACT

This project presents a comprehensive methodology for estimating the conducted electromagnetic interference (EMI) in switched-mode power supplies (SMPS). The primary focus is on developing a circuit model that forecasts conducted disturbances through both time and frequency domain simulations. The study utilizes LTspice software to model a power supply topology consisting of a high-voltage converter operating in discontinuous conduction mode (DCM) and a low-voltage converter operating in continuous conduction mode (CCM).

Additionally, the project includes the automation and optimization processes for Buck converters in three configurations: low-voltage, high-voltage, and double Buck converters. These processes were essential for streamlining the evaluation of their EMI performance, enabling rapid adjustment of parameters and achieving optimal design outcomes. Through a combination of direct and indirect simulation approaches, the research compares the accuracy and computational efficiency of these methods against experimental results obtained using the EMSCOPE device. The findings demonstrate the validity of frequency domain modeling for optimizing electromagnetic compatibility (EMC) filters, reducing the need for iterative prototype testing. The results indicate that the proposed methodology can effectively anticipate conducted disturbances, thereby enabling earlier and more efficient EMC filter design.

Contents

	Page
1 Introduction	18
1.1 Objectives	18
1.1.1 Ethics and health and safety at work	20
2 Literature Review	22
2.1 Reminder on Electromagnetic Compatibility	22
2.1.1 General	22
2.1.2 EMC Standards	23
2.1.3 Prescriptive measures and simulation	24
2.2 Continuous and Discontinuous Conduction of a Buck Converter	26
2.2.1 Description of a Buck Converter	26
2.2.2 Continuous conduction	28
2.2.3 Discontinuous conduction mode	29
2.3 Method for modeling conducted disturbances	31
2.3.1 Indirect methods: time domain simulation	31
2.3.2 Direct methods	33
3 Methodologies for modeling conducted disturbances	35
3.1 Modeling a Low Voltage Buck Converter	35
3.1.1 Continuous conduction Time Domain Modeling	35

	10
3.1.2	Continuous conduction Frequency Domain modeling 39
3.1.3	Comparison of the results of continuous conduction simulations 47
3.2	Modeling a High Voltage Buck Converter 50
3.2.1	Discontinuous conduction Time Domain Modeling 50
3.2.2	Discontinuous conduction Frequency Domain modeling 54
3.2.3	Comparison of the results of discontinuous conduction simulations 60
3.3	Modeling a Double Buck Converter 62
3.3.1	Time Domain Modeling 62
3.3.2	Frequency Domain Modeling 64
3.3.3	Comparison of the simulations results 67
4	Modeling methodology validation 69
4.1	Experimental phase-perturbation measurement 69
4.2	Comparison of Results 69
4.2.1	Low voltage Buck configuration 70
4.2.2	High voltage Buck configuration 72
4.2.3	Double Buck configuration 74
5	Automatizing and Optimization circuit Process 77
5.1	Automatizing 77
5.2	Optimization 79
6	Conclusions 83
7	Recommendations and prospects 84
References	86
Index	88

A 1. Behavior of LISN Model	88
B 2. Explanation of Common Mode (CM) Noise and Differential Mode (DM) Noise	91

List of Figures

1.1	Topology of a power supply type.	19
2.1	EMC Emission and Susceptibility [2].	23
2.2	CISPR/EN 55022/32 Class A and B Emission limits [1].	24
2.3	Circuit of two LISN for normative disturbance measurements conducted [2].	25
2.4	Converter topologies (a)Buck, (b)Boost, (c)Buck-Boost, (d)Cuk [6].	27
2.5	ON and OFF state of a buck converter in CCM [5].	28
2.6	Waveform in continuous conduction mode [5].	28
2.7	ON and OFF state of a buck converter in DCM [5].	30
2.8	Waveform in Discontinuous conduction [5].	30
2.9	Algorithm describing the steps of an indirect approach modeling	32
3.1	Simulated Time domain structure of a Low Voltage Buck Converter in Continuous Conduction.	36
3.2	Perturbation spectrum extracted with the function '.four' in continuous conduction of VLISN1 (Phase).	38
3.3	Perturbation spectrum extracted with the function '.four' in continuous conduction of VLISN2 (Neutral).	38
3.4	Perturbation spectrum extracted with the function '.four' in continuous conduction of Differential Mode Voltage(DM).	39
3.5	Perturbation spectrum extracted with the function '.txt' in continuous conduction of Common Mode Voltage (CM).	39

3.6 a. Diagram of the time domain representation b. First configuration of Frequency domain structure c. Second configuration of frequency Domain structure [8].	40
3.7 Modeling of the switching cell by equivalent generators [2].	41
3.8 Two different topologies with respect to the midpoint of the equivalent generators [2].	41
3.9 Idealized waveform through trapezoidal approximation in VDS and IMOS.	44
3.10 Simulated Frequency domain Structure of a Buck Converter in Continuous Conduction.	45
3.11 Spectrum extracted in continuous conduction of VLISN1 (Phase) Frequency Domain.	46
3.12 Spectrum extracted in continuous conduction of VLISN2 (Neutral) Frequency Domain.	46
3.13 Spectrum extracted in continuous conduction of Differential Mode (DM) Frequency Domain.	47
3.14 Spectrum extracted in continuous conduction of Common Mode (CM) Frequency Domain.	47
3.15 Comparison of Ids by Time and Frequency approach.	48
3.16 Comparison of Vd by Time and Frequency approach.	48
3.17 Comparison of VLISN1 (Phase) in Time and Frequency approach.	49
3.18 Comparison of VLISN2 (Neutral) in Time and Frequency approach.	49
3.19 Comparison of Differential mode (DM) in Time and Frequency approach.	49
3.20 Comparison of Common Mode (CM) in Time and Frequency approach.	50
3.21 Time domain Structure of a High Voltage Buck Converter in Discontinuous Conduction Mode.	51
3.22 Perturbation spectrum extracted with the function ".four" in Discontinuous conduction of VLISN1 (Phase).	53

3.23 Perturbation spectrum extracted with the function ".four" in Discontinuous conduction of VLISN2 (Neutral)	53
3.24 Perturbation spectrum extracted with the function ".four" in Discontinuous conduction of Differential Mode Voltage (DM)	53
3.25 Perturbation spectrum extracted with the function '.txt' in discontinuous conduction of Common Mode Voltage (CM)	54
3.26 a. Diagram of the time domain representation b. First configuration of Frequency domain structure c. Second configuration of frequency Domain structure.	55
3.27 Time domain representation of $VDS(t)$ and $IMOS(t)$ used in the Laplace transform expressions (DCM)	58
3.28 Simulated Frequency Domain structure of a buck converter in Discontinuous conduction Mode.	59
3.29 Comparison of Differential Mode(DM) - Time domain Mode vs Frequency Domain.	60
3.30 Comparison of Common Mode (CM) - Time domain Mode vs Frequency Domain.	60
3.31 Comparison of Source ID - Time domain Mode vs Frequency Domain.	61
3.32 Comparison of Source VD - Time domain Mode vs Frequency Domain.	61
3.33 Comparison of Differential Mode(DM) - Time domain Mode vs Frequency Domain.	62
3.34 Comparison of Common Mode (CM) - Time domain Mode vs Frequency Domain.	62
3.35 Time domain Modeling of the double buck converter structure.	63
3.36 Time domain spectrum of double buck Differential Mode (DM)	64
3.37 Time domain spectrum of double buck Common Mode (CM)	64
3.38 Diagram of the time domain representation.	65
3.39 Diagram of the Frequency domain representation.	65

3.40	Diagram of the Frequency domain representation.	66
3.41	Extraction of the waves of differential Mode in Frequency Domain.	66
3.42	Extraction of the waves of Common Mode in Frequency Domain.	67
3.43	spectrum of the Frequency domain vs Time domain voltages of Differential Mode.	68
3.44	spectrum of the Frequency domain vs Time domain voltage of Common mode. .	68
4.1	Generation of the measure data with EMSCOPE and connection of low voltage buck converter.	70
4.2	Diagram of the Frequency domain representation with measurement data . .	71
4.3	Diagram of the Frequency domain representation with measurement data. .	71
4.4	Generation of the measure data with EMSCOPE and connection of high voltage buck converter	72
4.5	Diagram of the Frequency domain representation with measurement data. .	73
4.6	Diagram of the Frequency domain representation with measurement data. .	73
4.7	Generation of the measure data with EMSCOPE and connection of double buck converter.	74
4.8	Diagram of the Frequency domain representation with measurement data. .	75
4.9	Diagram of the Frequency domain representation with measurement data. .	75
5.1	Automatizing tool for circuit analysis in frequency domain	78
5.2	Optimization process to identify all stray elements. The EMC frequency models are included into an optimization loop to identify the model parameters, thanks to a comparison between measured and conducted EMI	80
5.3	Result before the optimizing process	82
5.4	Result after the optimizing process	82
A.1	Model of LISN.	88

A.2 Frequency behaviour of the input impedance of LISN.	89
A.3 Model of LISN high side (Blue), low side (yellow).	89
B.1 Common Mode and Differential Mode propagation path [17].	93

List of Tables

2.1	LISN Structure	26
3.1	Parameters of Marked Components	37
3.2	Computation Time between Frequency Domain simulation and Time Domain simulation - Low Voltage Buck Converter	50
3.3	Parameters of Marked Components	52
3.4	Computation Time between Frequency Domain simulation and Time Domain simulatio - HIgh Voltage Buck Converter	61
3.5	Computation Time between Frequency Domain simulation and Time Domain simulatio - Double Buck Converter	68

Chapter 1

Introduction

Until now, the design phase of power electronics devices has been carried out without an effective means to predict electromagnetic disturbances. Only once the device has been completed and pre-certification tests have been conducted is it possible to determine the levels of conducted interference and, consequently, the appropriate EMC filter to reduce these disturbances. In this regard, a methodology for the rapid estimation of the disturbance spectrum would allow for the preliminary sizing and optimization of EMC filters to reduce conducted disturbances.

1.1 Objectives

The objective of this study is to define a methodology to estimate the conducted disturbance spectrum for switched-mode power supplies. This means that the design and optimization of EMC filters can be anticipated as early as the design phase. In EMC, two main families of models compete with each other in terms of their advantages and disadvantages: direct approach modeling and indirect approach modeling. The indirect approach involves simulating a system in the time domain and applying a Fourier transform to the resulting waveforms to obtain the spectrum. The direct approach involves performing calculations directly in the frequency domain. This approach is often preferred for optimization because it has a very low computational cost. In this study, the frequency modeling method of the transfer

function was chosen. In fact, the modeling of disturbance sources and the implementation of propagation paths remain intuitive within the framework of LTSpice following the direct approach. The objective of the work carried out was to model a power topology as shown in Figure 1.1 .

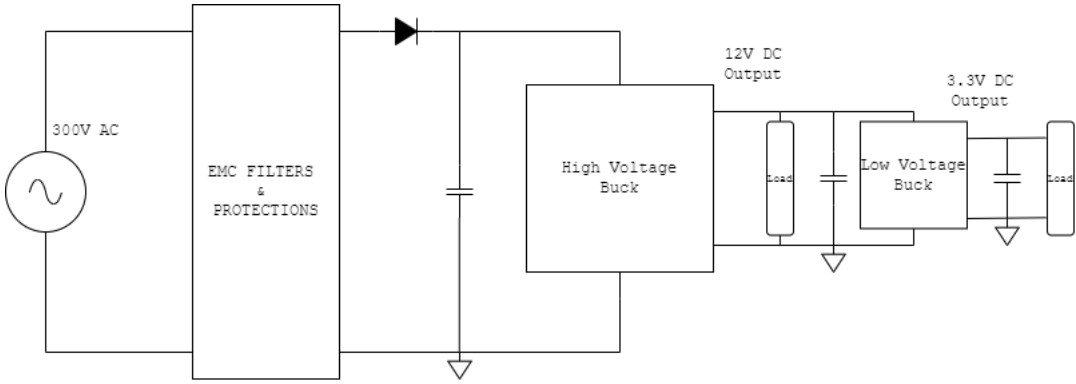


Figure 1.1: Topology of a power supply type.

In fact, this power supply includes a high-voltage converter (300V DC to 12V DC) that operates in discontinuous conduction mode and a low-voltage converter (12V DC to 3.3V DC) that operates in continuous conduction mode. Therefore, this study presents the details of the implementation of frequency domain modeling under LTSpice for Buck converters operating in both continuous and discontinuous conduction modes. A comparison was made between the simulation results (direct and indirect approaches) and the experimental results. This has allowed for highlighting the frequency validity domain of the established models.

Including a program where the LTspice software will be automated, allowing us to modify the parameters of Buck converters and obtain their frequency response for future analyses following rigorous criteria. Additionally, this will enable the optimization of these converters to approximate as closely as possible to our measurements performed with EMSCOPE.

EMSCOPE is an advanced instrument used for electromagnetic compatibility (EMC) testing and analysis. It allows for precise measurements of electromagnetic interference

(EMI) and helps in diagnosing and mitigating potential issues in electronic circuits. By providing detailed insights into the EMC performance, EMSCOPE plays a crucial role in ensuring that electronic devices meet regulatory standards and function reliably in various environments.

1.1.1 Ethics and health and safety at work

Sustainable development

This study has made it possible to establish a fast and less expensive approach to modeling perturbations. As the environmental issue is a priority at Somfy, this methodology will allow the designer to reduce the number of prototypes designed and developed. With this approach, optimizing the footprint of EMC filters is possible, thus avoiding the oversize filter design.

Ethics

Simulation-based approaches are often welcomed by some and rejected by others. Indeed, very often, the other side of the calculation methods is unknown to users. Thus, instead of providing a tool that has already been implemented, this study proposes a method of approach, thus allowing a designer to build and control his design.

Health and Safety

On the one hand, during this study, the vast majority of the work was carried out in simulation, which represents several hours in front of a screen. Appropriate provisions have been made available in this context. Also, training on good practices to adopt when you

are behind a workstation was provided. On the other hand, during the anechoic chamber measurement phases, the provisions and training relating to electrical risks were applied in order to prevent any risk of danger. For example, an electrical accreditation training course (delivered by SOCOTEC) was carried out at the beginning of the internship, detailing the various risks existing within the Somfy R&D Center. During the measurements carried out with voltages of 300V, the electronic boards were placed under an insulating envelope to prevent risks. In addition, fire simulations are carried out regularly to familiarise employees with the evacuation procedure.

Chapter 2

Literature Review

2.1 Reminder on Electromagnetic Compatibility

2.1.1 General

Electromagnetic compatibility is a field that aims to study the problems related to electromagnetic cohabitation [1]. According to the international electrotechnical vocabulary VIE 161-01-07, EMC is the ability of an electronic device, equipment or system to function satisfactorily in its electromagnetic environment without introducing electromagnetic disturbances intolerable for anything in that environment [1].

"Emission and Susceptibility" are two key words to understand EMC. Emission represents the ability of a device to transmit electromagnetic disturbances by conduction or radiation to its surroundings. Susceptibility refers to the ability of that same device to be disturbed by its electromagnetic environment. These terms allow us to define the three basic notions of Electromagnetic Compatibility analysis, which are: Sources, Paths and Victims as presented in Figure 2.1.

¹ It is important to note that there is always a level of disturbance generated by a device or environment. This is the reason why standards have been defined for limiting conducted and radiated disturbances, which vary from one field to another depending on the

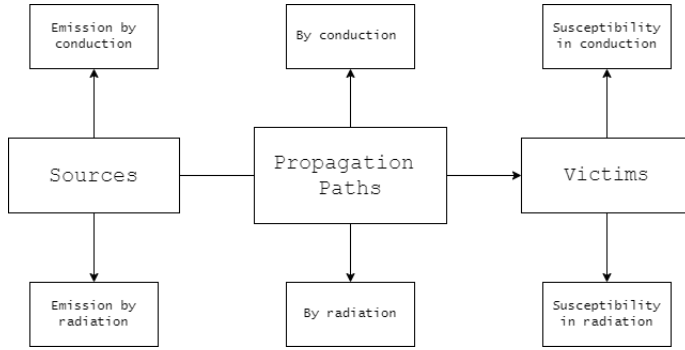


Figure 2.1: EMC Emission and Susceptibility [2].

device or system developed. In power electronics, the main sources of conducted disturbances are due to sudden changes in the states of the converter's power switches. These sudden changes cause rapid variations in current or voltage across the various components [3].

2.1.2 EMC Standards

The analysis of EMC problems is guided by European and international standards that will dictate the marketing of electrical equipment. In the civil field, EMC standards define disturbance levels that must not be exceeded over a frequency band of 150kHz-30MHz for conducted disturbances and 10kHz-18GHz for radiated disturbances. The standards for the disturbances conducted will vary from one product to another depending on the country of implementation and the case of application.

As an example for Somfy products, a European standard that defines the EMC test methods and limits to be complied with is the CISPR EN 55032 standard (Figure 2.2). This standard is defined by the International Special Committee on Radio Interference (CISPR). It defines global agreements on electromagnetic interference in a way that simplifies international trade. For the American continent, FCC standards are applied. The difference between these two categories of standards lies in the limits to be respected. The prescriptive

test methods remain broadly the same for both. As Somfy is a multinational, it must apply the standard relating to the country where its products will be used. Compliance with standards is often a guarantee of the quality and competitiveness of manufacturers' products. These standards are generally classified into two groups: 1. Conducted and radiated emission level and 2. Equipment susceptibility level.

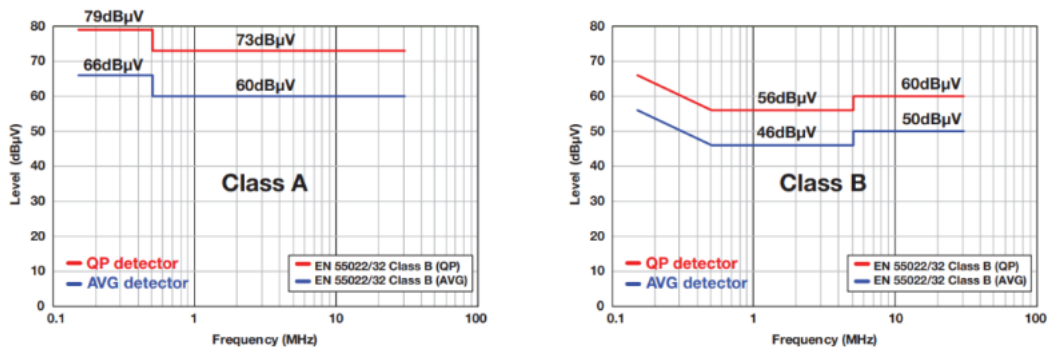


Figure 2.2: CISPR/EN 55022/32 Class A and B Emission limits [1].

The standards also set out the methods for measuring and interpreting results. In general, disturbance levels should be defined on a normative logarithmic scale in dB μ V. Thus, this will be the scale used for all spectral analyses in this report.

$$\text{dB}\mu\text{V}(V) = 20 \log_{10} \left(\frac{V}{10^{-6}} \right) \quad (2.1)$$

Equation 2.1 : conversion V to dB μ V

2.1.3 Prescriptive measures and simulation

For conducted disturbances, the measuring device will depend on the current level absorbed by the equipment under test (EST). For line currents below 100A (which is the case of this study), it will be necessary to use the Line Impedance Stabilizer Network (LISN). The

LISN is a device for defining a stable characteristic impedance of the measuring branches over the entire normative frequency range (150kHz-30MHz) for conducted disturbances. It thus makes it possible to validate the reproducibility of the measurements and to partially set the measurement conditions. There are different structures of LISN depending on the field of application. The fact remains that everyone must respect an impedance of 50Ω over the analysis frequency range (150kHz-30MHz). This value allows impedance matching with measuring devices such as the spectrum analyzer [4]. Figure 2.3 shows the overall structure of the LISN in the context of a conducted disturbance measurement.

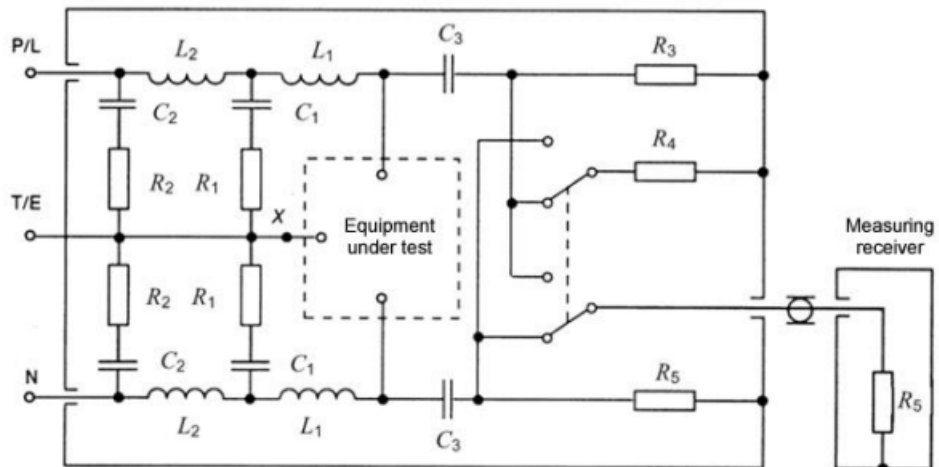


Figure 2.3: Circuit of two LISN for normative disturbance measurements conducted [2].

L2, C2, R2, C3, R3 and RLISN (Table 2.1 and Figure 2.3) make up the structure of a single LISN. There are different models of LISN depending on the frequency range you want to study. Thus, the values of the components and the structure adopted were defined according to the normative band of the emission measurements conducted and the number of components [5]. Indeed, a more complex structure of LISN increases the calculation times of the simulations and does not change anything in terms of the simulation measurements on the normative emission band conducted.

Table 2.1: LISN Structure

Component	Value
R_1	5 Ω
R_2	10 Ω
R_3	1 000 Ω
R_4	50 Ω
R_5	50 Ω (input impedance the measuring receiver)
C_1	8 μF
C_2	4 μF
C_3	0.25 μF
L_1	50 μH
L_2	250 μH

In simulation, power source faults are partially considered through line impedances. Therefore, a simplified structure of the LISN was used. The latter has a satisfactory frequency behavior (Appendix 2.) on the study frequency band (150kHz-30MHz). This simplified structure therefore reduces the calculation load of the simulator [4].

2.2 Continuous and Discontinuous Conduction of a Buck Converter

2.2.1 Description of a Buck Converter

Figure 2.4 shows the most common converter topologies for power supplies, which are Buck, Boost, Buck-Boost, and Cuk [6].

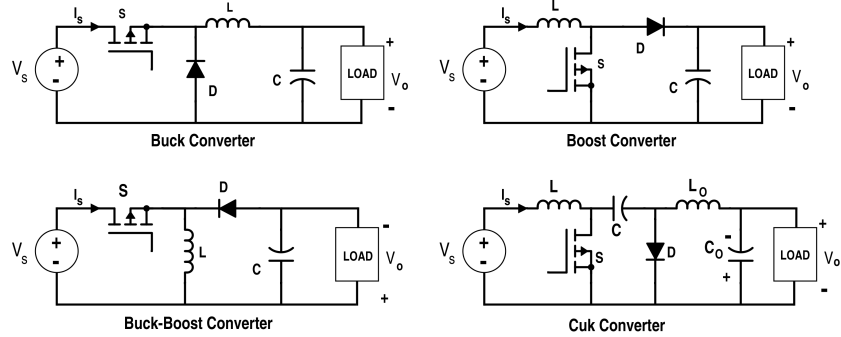


Figure 2.4: Converter topologies (a)Buck, (b)Boost, (c)Buck-Boost, (d)Cuk [6].

A buck converter consists of DC (V_s) or rectified AC power supply, a switch (transistor-S), a freewheeling diode (D), a low-pass filter (LC), and the load. The buck topology is typically used for systems that require DC power. Designers often opt for the topology of a Buck when it is necessary to have an output voltage (V_o) that is lower than the input voltage and that is not isolated from the input (i.e., the output and input voltage share a common ground plane).

During normal operation of a buck converter, the S switch opens and closes repetitively according to a control voltage V_g that drives the gate of a transistor. When S is closed, a current flows from the source to the load through S. However, when S is open, the current stored in the output inductor flows to the load through the freewheeling diode D. In this study, the type of transistor used for measurement and simulation was NMOS transistors due to the fact that they are faster and have a relatively low $R_{DS(on)}$. This minimizes losses at the switch [5].

A buck converter can be operated in two conduction modes: Continuous Conduction (CCM) and Discontinuous Conduction (DCM). These modes of operation are described in detail in [6] and are discussed briefly in the following sections.

2.2.2 Continuous conduction

In continuous conduction, the buck converter admits two operating states: 1.ON-state and 2.OFF-state. The ON-state phase occurs when the Pch FET switch is closed and the Nch FET switch is open as shown in Figure 2.5. The OFF-state is when the Pch FET switch is open and the Nch FET switch is closed (also called the freewheeling phase). Figure 2.6 shows the theoretical waveforms appearing in continuous conduction [5].

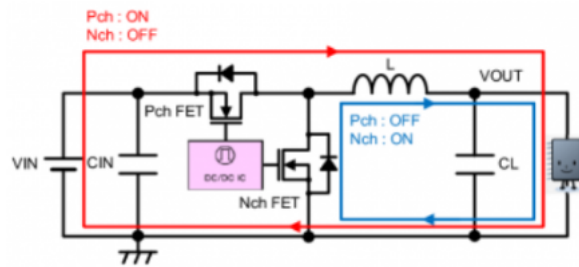


Figure 2.5: ON and OFF state of a buck converter in CCM [5].

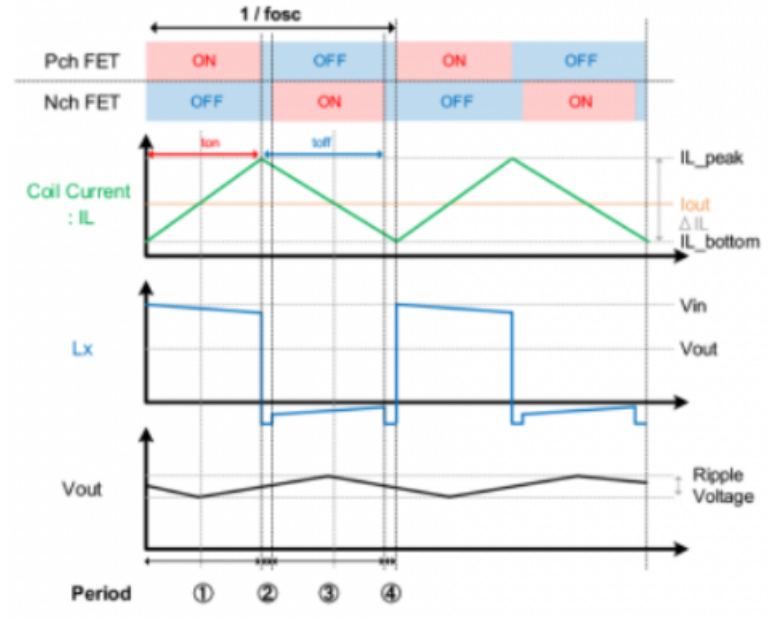


Figure 2.6: Waveform in continuous conduction mode [5].

In continuous conduction, the load current is large enough to allow a direct flow of

current through the inductor. In other words, the current through the output inductance is never zero. The TON duration defines the time for which Pch FET is closed and TOFF defines the time for which Nch FET is closed. These durations are defined by a parameter called the duty cycle. The duty cycle is defined as the ratio between the time at high state (TON) of a signal and its period [5]. In continuous conduction, the output voltage is directly proportional to the product of the duty cycle and the input voltage as described in the following equation 2.2:

$$V(\text{out}) = \text{Duty Cycle}(D) \times V(\text{in}) \quad \text{where } D = \frac{T_{\text{ON}}}{T_{\text{ON}} + T_{\text{OFF}}} \quad (2.2)$$

Equation 2.2: Relationship between output voltage and duty cycle in continuous conduction.

2.2.3 Discontinuous conduction mode

Unlike continuous conduction, discontinuous conduction has three operating states. In addition to the two (ON-state and OFF-state) states described for continuous conduction, there is a third state called IDLE-state (inactive) during which both Pch FET and Nch FET are open (Figure 2.7). In the IDLE phase, there is only a leakage current that flows to the load through the parasitic capacitance CL of the Pch FET transistor. In discontinuous conduction mode, the charging current is not large enough to allow a continuous flow of current through the inductor (IL in Figure 2.8). The red rectangle indicates the discontinuity of the current through the output inductor, which is almost 0A for a fraction of the period [5].

This time, the output voltage is no longer only proportional to the duty cycle (D) as presented in equations 2.3 and 2.4.

Equation 2.3 : Relationship Between Output Voltage and Duty Cycle in Discontinuous

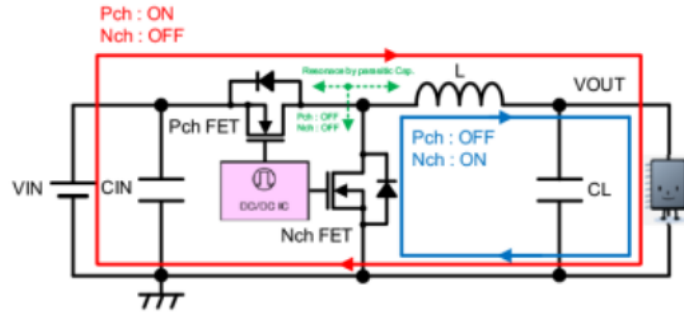


Figure 2.7: ON and OFF state of a buck converter in DCM [5].

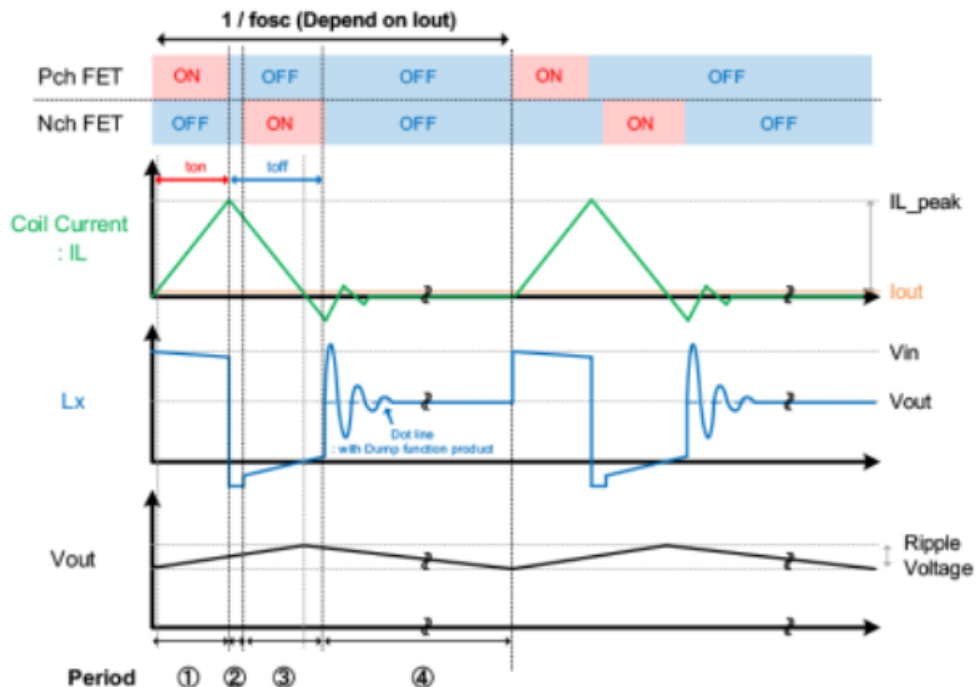


Figure 2.8: Waveform in Discontinuous conduction [5].

Conduction.

$$V(\text{out}) = V(\text{in}) \times \frac{2}{1 + \sqrt{1 + \frac{4 \times \left(\frac{2L}{R \cdot T_{\text{off}}}\right)}{D^2}}} \quad (2.3)$$

Here is the breakdown of each element in the equation:

- $V(\text{out})$: The output voltage of the system.
- $V(\text{in})$: The input voltage to the system.
- L : The output inductance in the circuit.
- R : The output resistance in the circuit.
- T_{off} : The off-time of the switching cycle.
- D : The duty cycle, which is the ratio of the on-time to the total time period of the switching cycle.

where:

Equation 2.4: Formula of duty cycle in Discontinuous conduction Mode

$$D = \sqrt{\frac{2 \times L_{\text{output}} \times f_d \times I_{\text{output}}}{V_{\text{input}} \left(\frac{V_{\text{input}}}{V_{\text{output}}} - 1 \right)}} \quad (2.4)$$

2.3 Method for modeling conducted disturbances

The objective of EMC modeling is to be able to transcribe the different couplings that can appear with maximum plausibility.

2.3.1 Indirect methods: time domain simulation

The indirect approach consists of performing a time domain simulation of the behavior of a system and then performing a Fourier transform on the desired signals to obtain the

spectra. This method makes it possible to simulate the inherent non linearity's of a circuit. However, it remains poorly suited for simulations taking into account parasitic elements, time constants introduced by LISN and loading. This is due to the fact that time domain simulation requires a very large number of simulation points for complex structures if the model is to be exploitable [5]. Figure 2.9 presents an algorithm describing the steps involved in indirect approach modeling.

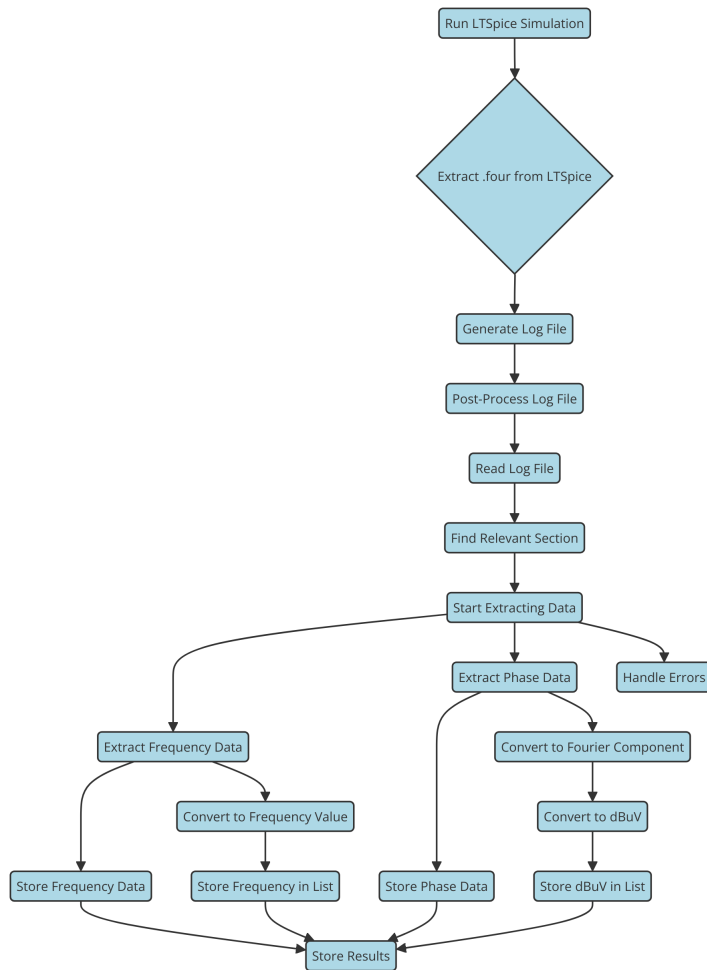


Figure 2.9: Algorithm describing the steps of an indirect approach modeling

However, time domain simulation remains an effective analytical tool for the functional validation of electrical systems. However, it remains poorly suited for automatic optimization due to very long computation times and convergence problems. All the simulation

are taking into account the Shannon criteria [2].

2.3.2 Direct methods

Direct methods, on the other hand, consist of carrying out simulations directly in the frequency domain. However, these types of methods require more hindsight than indirect methods. The mechanisms of perturbation generation as well as all propagation paths must be well understood to arrive at a representative frequency domain modeling [3].

To perform frequency domain modeling, two steps are necessary:

1. **Identification and linearization of disturbance sources.**
2. **Definition of propagation paths.**

Nowadays, many modeling techniques directly in the frequency domain have been developed. A previous work proposed a comparison regarding the different modeling techniques [2].

The frequency domain method presents a non-negligible advantage in terms of calculation speed, suitable for iterative calculations for optimization. In this type of modeling, several assumptions are made:

1. **Linear behavior of disturbance sources.**
2. **Simulation performed only in steady-state and one single operation point.**
3. **Switches are idealized and thus the waveforms at their terminals are perfect trapezoidal or triangular without oscillations at the opening and closing of the switches.**

4. Disturbance sources are independent of propagation paths.

Following these assumptions, the disturbance sources are replaced by linearized equivalent generators. This step can thus cause a certain number of inaccuracies in the calculation of the disturbance spectrum. Moreover, frequency domain simulations are often preceded by phases of equation formulation and analytical development which can be sometimes long and complex.

In this study, as the implementation of the frequency domain models was carried out on LTspice, the method adopted was inspired by the transfer function approach [7]. This method allows to define a global frequency domain structure without separation of common and differential mode propagation paths. The fact that LTSpice allows to implement transfer functions guided the choice of this modeling approach.

Chapter 3

Methodologies for modeling conducted disturbances

As mentioned earlier, in order to determine the validity of implementations of a frequency domain model under LTSpice, the results of frequency domain simulation were compared with the results of time domain simulation and measurement. Therefore, this section describes the implementation of time domain and frequency domain modeling of a buck converter according to the two conduction modes CCM and DCM. Then, the measurement benches and the results obtained are developed before a comparison of the different simulation and measurement results [2].

3.1 Modeling a Low Voltage Buck Converter

3.1.1 Continuous conduction Time Domain Modeling

Time Domain structure in continuous conduction Mode

In order to confirm the implementation of a frequency domain model under LTspice, a first phase of time domain simulation of a Buck converter in continuous conduction was performed. The objective is to be able to validate the simulation results of frequency domain modeling

by comparing them to the spectra obtained by indirect approach. The following Figure 3.1 shows the time domain structure of a Buck converter operating in simulated LTspice CCM.

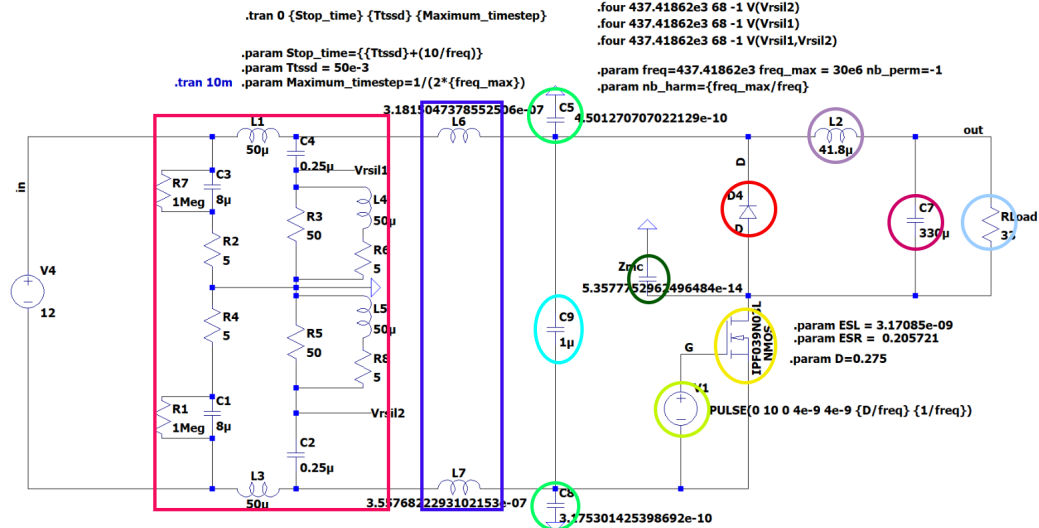


Figure 3.1: Simulated Time domain structure of a Low Voltage Buck Converter in Continuous Conduction.

To reach this time domain structure, a functional validation step was implemented as described in a previous work [2]. This step enabled us to understand the behavior of a buck converter in continuous conduction, as well as the influence of various components. This approach complements the results measured with the EMSCOPE device.

The structure in Figure 3.1 accounts for the parasitic elements of each component, which are detailed in the following table 3.1 along with their respective descriptions.

Table 3.1: Parameters of Marked Components

Component	Characteristic
LISN	The simplified structure of the LISN with an acceptable frequency behavior over the frequency range studied.
L6, L7	Represents a cable between the LISN and the power converter with an inductance of $1\mu\text{H}/\text{m}$ of cable
C5, C6	Represents the capacitance's of the prototype PCB model
C9	Input capacitor of $1\mu\text{F}$ with $\text{ESR}=0.2057\Omega$ and $\text{ESL}=3.17085\text{ nH}$
Zmc	A common-mode impedance= 0.05357pF that models the impedance between the ground plane of the converter and that of the EMSCOPE setup.
MOSFET	NMOS transistor IPF039N03L that acts as a switch for the buck converter topology.
D4	Represents an ideal freewheeling diode
L2	Output inductance of $41.8\mu\text{H}$ with $\text{ESR}=1.05\Omega$.
C7	$330\mu\text{F}$ output capacitor of the LC filter with a $\text{ESR}=115\text{m}\Omega$
Rload	Output ideal resistor with a value of $= 33\Omega$ to reach the operating point of the prototype.

Extraction of the disturbance spectrum from Time Domain Simulation.

In Figure 3.1, it can be noted that the ".four" function under LTspice was used on the VLISN1(Phase), VLISN2(Neutral), Differential Mode, voltages in order to obtain the spec-

trum of multiple harmonics of the switching frequency (switching frequency = 437.418kHz). The use of this function makes it possible to obtain the amplitudes of these harmonics. Indeed, only these frequencies will be able to carry energy and thus contribute to the conducted EMI.

Thus, the spectrum obtained is consistent over the frequency range specified by the conducted disturbance standards (150kHz - 30MHz). Figure 3.2, 3.3 and 3.4, shows the spectrums obtained from VLISN1, VLISN2, Differential Mode.

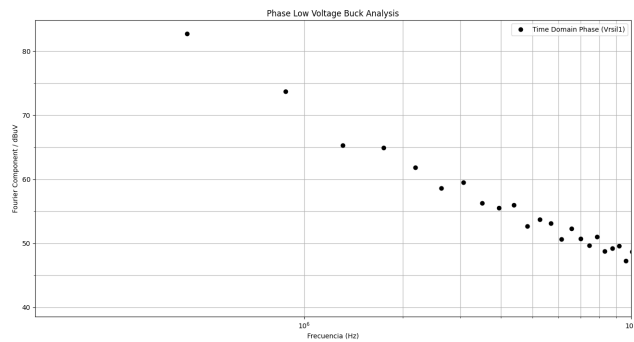


Figure 3.2: Perturbation spectrum extracted with the function '.four' in continuous conduction of VLISN1 (Phase).

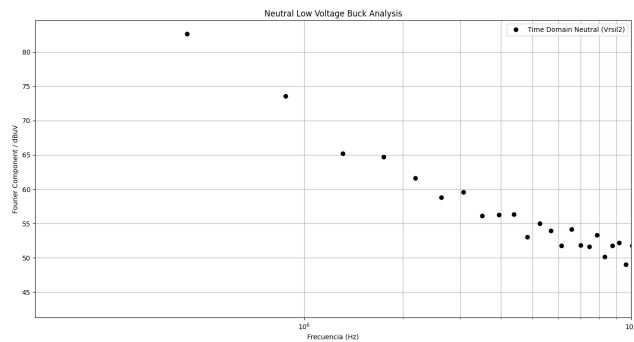


Figure 3.3: Perturbation spectrum extracted with the function '.four' in continuous conduction of VLISN2 (Neutral).

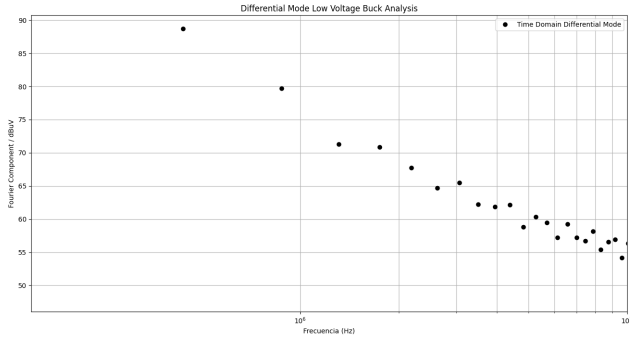


Figure 3.4: Perturbation spectrum extracted with the function '.four' in continuous conduction of Differential Mode Voltage(DM).

A very different method is used for obtaining the Common Mode since we do not have any nodes provided by LTspice to apply the ".Four" analysis. We use the program's "FFT" function where we calculate $\frac{VLISN1+VLISN2}{2}$. The obtained spectrum is converted to .txt format and its information is post-processed to obtain the Common Mode values, shows in Figure 3.5.

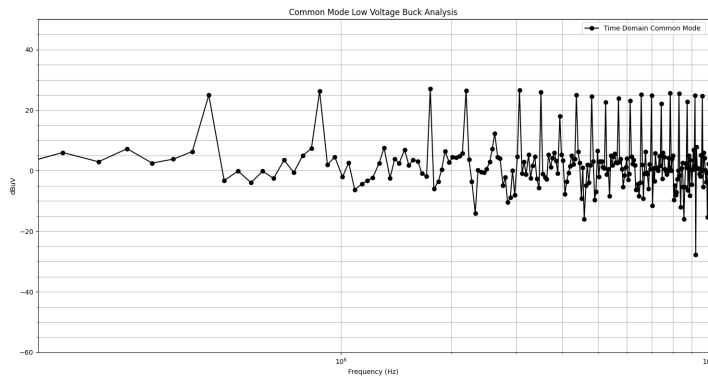


Figure 3.5: Perturbation spectrum extracted with the function '.txt' in continuous conduction of Common Mode Voltage (CM).

3.1.2 Continuous conduction Frequency Domain modeling

As mentioned earlier, to perform frequency domain modeling, two criteria are needed:

1. Identification and linearization of disturbance sources

2. Identification of propagation paths

The objective is to be able to achieve the frequency domain structure presented in Figure 3.6.

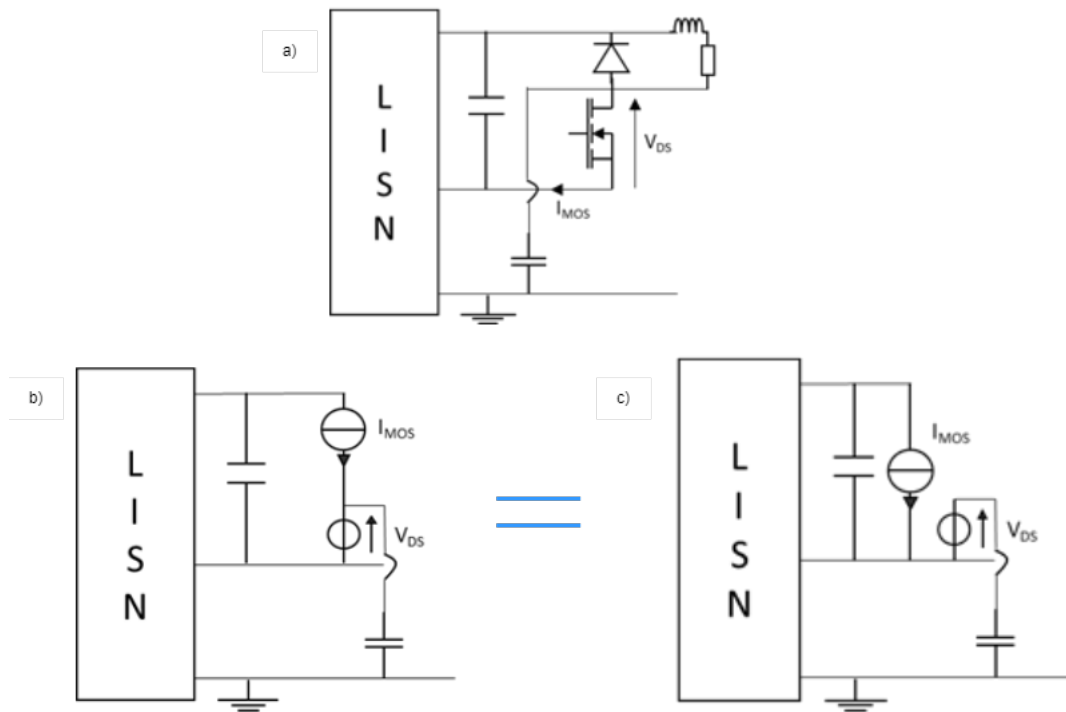


Figure 3.6: a. Diagram of the time domain representation b. First configuration of Frequency domain structure c. Second configuration of frequency Domain structure [8].

Modeling of disturbance sources

As mentioned earlier, the first step is to perform a modeling of the sources of disturbance. The EMC problem in the design of power converters defines the cell as a "source" of dis-

turbance [3]. Conventional modeling consists of modeling the switching cell by equivalent generators as shown in Figure 3.7.

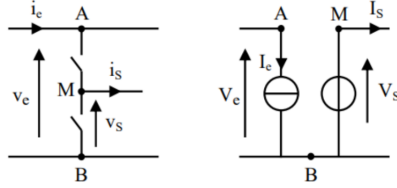


Figure 3.7: Modeling of the switching cell by equivalent generators [2].

These equivalent generators take into account the influence of the load and the source through the different parameters of their equation [2]. However, in this type of modeling, it is important to consider the location of the generators as this is what will determine the characteristics of the voltage generator V_s and the topology of the linearized frequency domain model.

For this, two options are possible. Indeed, one could choose to place V_s to model V_T (voltage across the transistor) or V_d (voltage across the freewheeling diode) as shown in Figure 3.8.

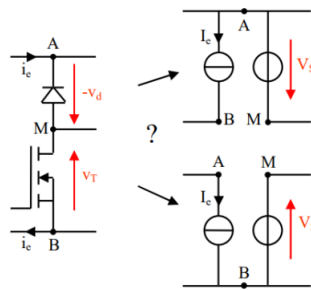


Figure 3.8: Two different topologies with respect to the midpoint of the equivalent generators [2].

Both topologies can be chosen as they will both undergo the discontinuities due to switching. However, when making this choice, it is important to note the change in circuit

topology with respect to the midpoint 'M' of the switching cell. In our study, the modeling of V_T by V_S ($V_S = V_T$) is chosen.

Once this choice is made, it is now necessary to define these sources of disturbances I_{MOS} and V_{DS} . The chosen method consists of linearizing the behavior of the converter through a trapezoidal approximation of the voltage V_{ds} (V_{DS}) of the transistor and the current I_d (I_{MOS}) flowing through the transistor. For this approximation, the formulation in the Laplace domain was chosen because it remains simple to implement under LTspice allowed us to arrive at equations 3.1 and 3.2.

Let be the generic equation of the Laplace transform of a trapezoid shapes:.

Equation 3.1: Laplace transform of I_{ds} following a trapezoidal shape approximation.

$$I_{MOS}(s) = 2 \cdot f_{sw} \left[\frac{I_{pk} - \Delta I}{\text{tri} \cdot s^2} \cdot (1 - \exp(-s \cdot \text{tri})) \right. \\ \left. + \exp(-s \cdot \text{tri}) \cdot \frac{\Delta I}{(d \cdot T_{sw} - \text{tri} - t_{fi}) \cdot s^2} \cdot (1 - \exp(-s \cdot (d \cdot T_{sw} - t_{fi} - \text{tri}))) \right. \\ \left. - \exp(-s \cdot (d \cdot T_{sw} - t_{fi})) \cdot \frac{I_{pk}}{t_{fi} \cdot s^2} \cdot (1 - \exp(-s \cdot t_{fi})) \right] \quad (3.1)$$

- $I_{MOS}(s)$: Current through the MOSFET transistor, expressed as a function of s , which could be the complex variable used in Laplace analysis.
- s : Complex variable used in Laplace transforms, representing complex frequency.
- f_{sw} : Switching frequency of the transistor or associated circuit.
- I_{pk} : Peak current, representing the maximum current that the circuit can achieve.
- ΔI : Change or variation in current during a specific interval.

- tri : Rise time, the interval during which the current or signal rise from its minimum value to maximum value.
- d : Duty cycle of the transistor or circuit, a fraction of the total period during which the transistor is active.
- T_{sw} : Switching period, the total time for one complete switching cycle ($1/(f_{sw})$).
- t_{fi} : Fall time, the interval during which the current or signal falls from its maximum value to zero or a residual value.

Equation 3.2: Laplace transform of V_{ds} following a trapezoidal approximation.

$$V_{DS}(s) = 2 \cdot f_{sw} \left[\exp(-s \cdot \text{tri}) \cdot \frac{-V_{ds}}{t_{fv} \cdot s^2} \cdot (1 - \exp(-s \cdot t_{fv})) \right. \\ \left. + \exp(-s \cdot (d \cdot T_{sw} - t_{fi} - t_{rv})) \cdot \frac{V_{dc}}{t_{rv} \cdot s^2} \cdot (1 - \exp(-s \cdot t_{rv})) \right] \quad (3.2)$$

- $V_{DS}(s)$: Represents the drain-to-source voltage of the MOSFET as a function of s . This function typically involves the Laplace transform, indicating it describes how the voltage behaves in the frequency domain.
- s : Complex variable used in Laplace transforms, representing complex frequency.
- f_{sw} : Switching frequency of the transistor or associated circuit.
- tri : Rise time, the interval during which the current or signal rise from its minimum value to maximum value.
- V_{ds} : The peak or steady-state drain-source voltage across the MOSFET during operation. This voltage is crucial for determining the operating point and the efficiency of the device.
- t_{fi} : Fall time, the interval during which the current or signal falls from its maximum value to zero or a residual value.
- d : Duty cycle of the transistor or circuit, a fraction of the total period during which the transistor is active.
- T_{sw} : Switching period, the total time for one complete switching cycle ($1/(f_{sw})$).
- V_{dc} : Represents the DC voltage level applied to the circuit. This voltage is crucial for the operation of electronic circuits, especially in power electronics where DC voltages are converted to AC or different levels of DC.

The trapezoidal approximation does not take into account the high-frequency oscillations at the opening and closing of the NMOS as shown in Figure 3.9 . The advantage of this approximation is however a simple description of the behavior of the converter thus allowing to have an estimate of the real spectrum.

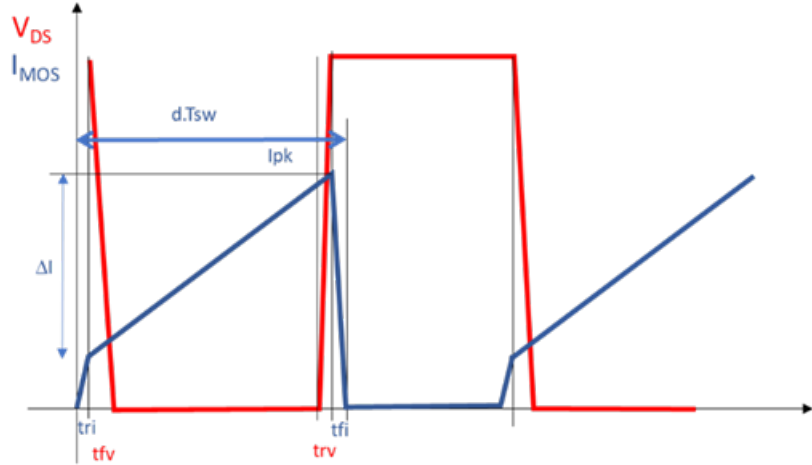


Figure 3.9: Idealized waveform through trapezoidal approximation in VDS and IMOS.

Implementing the Frequency Domain Structure in LTSpice

As elaborated above, for frequency domain modeling, the sources of disturbances are modeled by equivalent voltage and current generators. These generators are then defined by Laplace equations, thus allowing the linearization of their behavior. The equation in the form of a Laplace transform is performed in order to be able to perform the implementation and simulation directly in the frequency domain under LTSpice [9].

For a buck converter consisting of a single switching cell, the sources of disturbance are modeled as I_{ds} and V_{ds} (corresponding respectively to the current flowing through the NMOS switch and the voltage across the NMOS switch).

Their behaviors are approximated as perfect trapezoids (continuous conduction) and the waveforms are periodic square signals. In order to allow the implementation of the equations

defined previously under LTspice, voltage controlled voltage source (E1) and voltage controlled current sources (G1) are used as shown in Figure 3.10. Both are controlled by Laplace equations and correspond to the waveforms of MOSFET drain current (equation 3.1) and drain to source voltage (equation 3.2). These generators are excited by an AC voltage of 1V in order to allow the realization of a frequency domain simulation [1].

```
LAPLACE = 2*fd*(((Ipk - AI)/tr)/(s^2)*(1-exp(-tr*s)))+((exp(-tr*s)*(AI/Ton)/(s^2)*(1-exp(-s*Ton)))-((exp(-s*(Ton+tr)))*(Ipk/tf)/(s^2)*(1-exp(-s*tf))))  
LAPLACE = Vamp*(fd)^2*(1/(s^2))*(((1-exp(-s*tmv))/tmv)-((1-exp(-s*tdv))/tdv)*(exp(-s*((d)/fd)+(tmv/2)-(tdv/2))))*exp(-s*Ton)
```

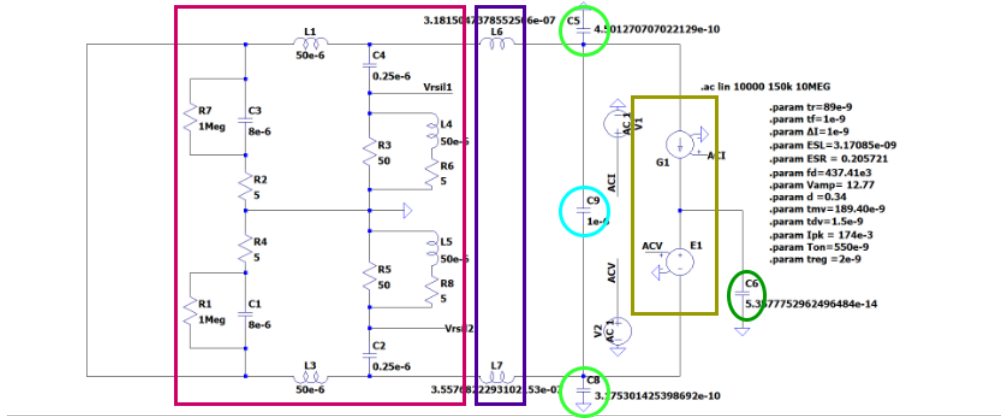


Figure 3.10: Simulated Frequency domain Structure of a Buck Converter in Continuous Conduction.

The implementation of Laplace's sources and equations has been validated according to the work carried out where it has been demonstrated that LTspice can be used to simulate frequency domain structures composed of linearized equivalent generators [2].

The advantage of using LTspice for frequency domain modeling is that propagation paths can be defined intuitively by arranging perturbation sources in series or parallel. In this way, we do not have to do with an analytical calculation phase of propagation paths and save a considerable amount of time. Indeed, a purely analytical frequency domain modeling would lead to complex transfer function calculations in order to model the overall impedance on which the sources of disturbance are reflected [9].

Extraction of the disturbance spectrum from Frequency Domain simulation

The frequency domain analysis begins with the setup and simulation of the circuit using LTspice, where each component is accurately placed according to the schematic provided.

Perform a frequency sweep analysis from 150 KHz to 10 MHz (to clearly obtain the data of interest for future analysis with the data measured on the implemented prototype) and save the output in a .raw file. After simulation, extract and process the data from this file using a specialized script, focusing on extracting voltage traces from the nodes of interest. These voltage values are then converted to microvolt decibels for clarity and ease of analysis. Subsequent steps involve plotting the frequency response for the critical nodes, including VLISN1, VLISN2, Differential Mode and Common Mode voltages, as shown in Figures 3.11, 3.12, 3.13 and 3.14.

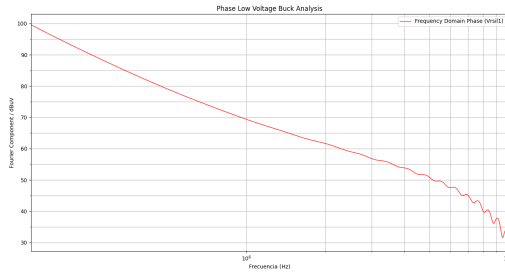


Figure 3.11: Spectrum extracted in continuous conduction of VLISN1 (Phase) Frequency Domain.

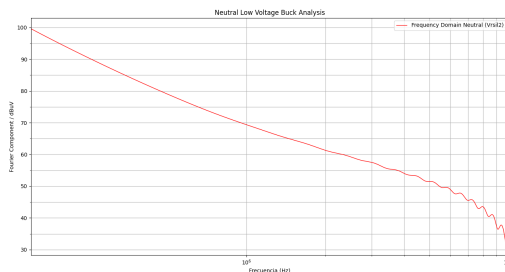


Figure 3.12: Spectrum extracted in continuous conduction of VLISN2 (Neutral) Frequency Domain.

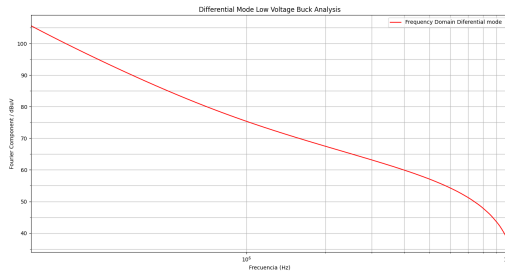


Figure 3.13: Spectrum extracted in continuous conduction of Differential Mode (DM) Frequency Domain.

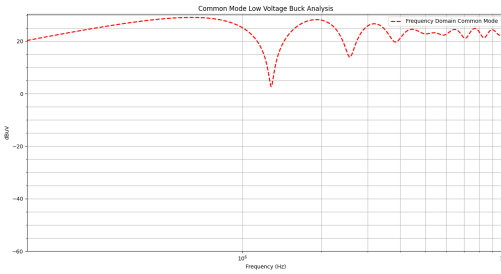


Figure 3.14: Spectrum extracted in continuous conduction of Common Mode (CM) Frequency Domain.

3.1.3 Comparison of the results of continuous conduction simulations

Before being able to compare the perturbation spectra, it is important to be able to validate the correct implementation of the equivalent generators. If, however, significant differences are identified at this level show in Figure 3.15 and 3.16, it is very likely that the two models are not at the same point of operation. It is important to check and confirm the values of the various parameters of the frequency domain modeling [9].

The spectrum of the signal of I_{ds} and V_{ds} agree well on the frequency range of 150kHz-5MHz. This frequency range of interest is enough for our study in the perspectives of a filter design. Moreover, the lowest the frequency of the EMI to filter, the biggest the size of the filter's passive components.

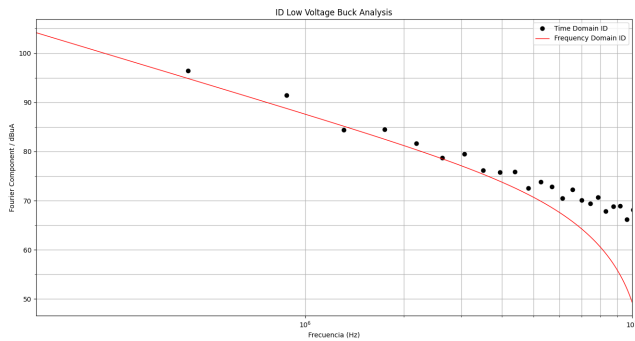


Figure 3.15: Comparison of Ids by Time and Frequency approach.

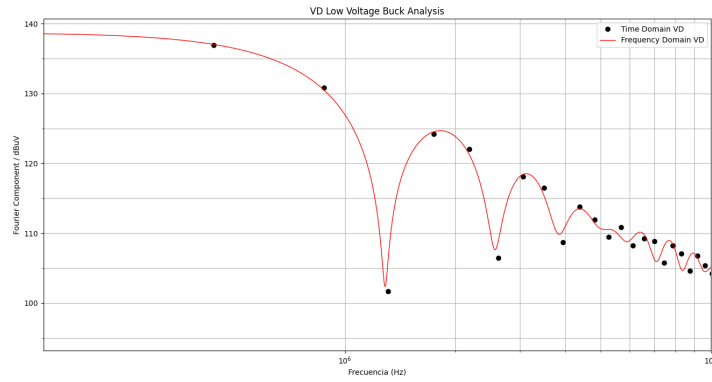


Figure 3.16: Comparison of Vd by Time and Frequency approach.

The advantage of frequency domain modeling is highlighted through very short simulation times shows in the Table 3.2. Indeed, with very low computation time between time domain modeling and frequency domain modeling we can obtain results like in the figure 3.17, 3.18, 3.19 and 3.20.

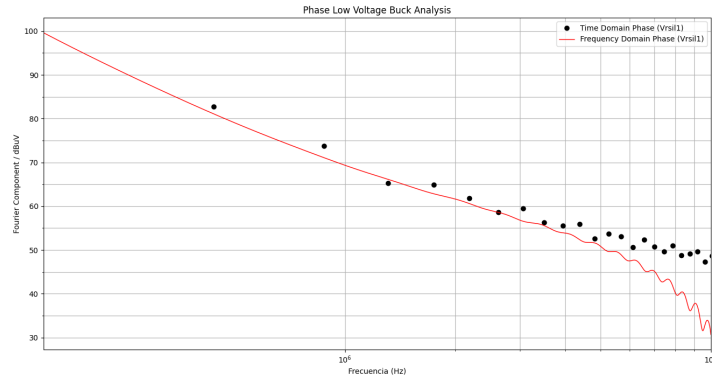


Figure 3.17: Comparison of VLISN1 (Phase) in Time and Frequency approach.

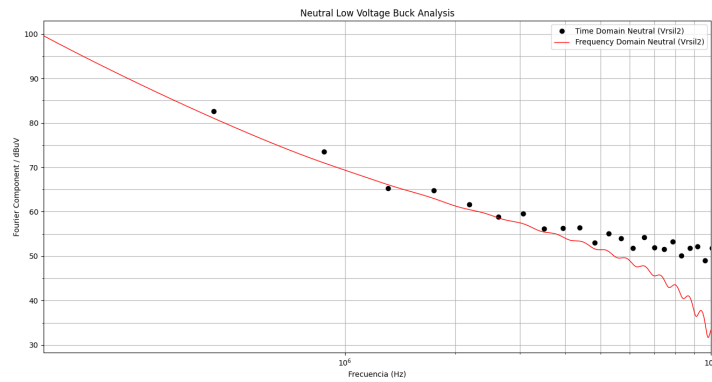


Figure 3.18: Comparison of VLISN2 (Neutral) in Time and Frequency approach.

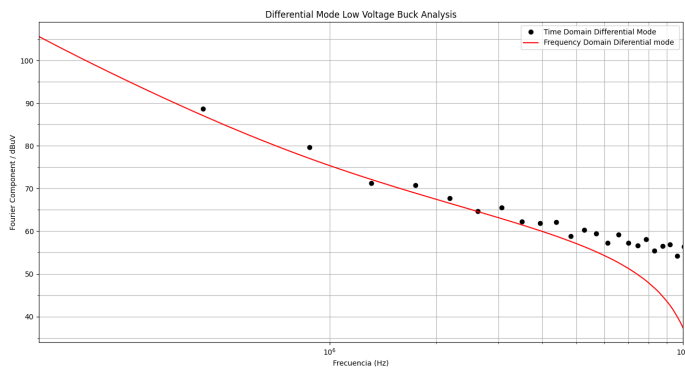


Figure 3.19: Comparison of Differential mode (DM) in Time and Frequency approach.

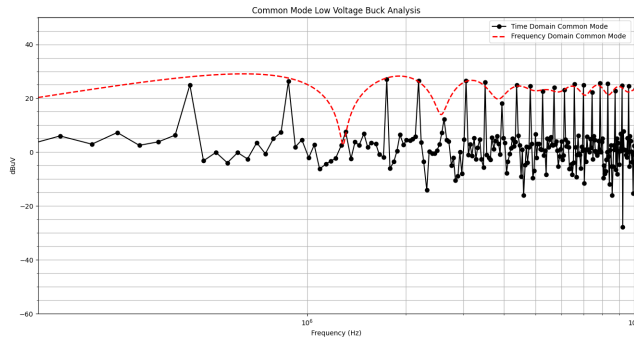


Figure 3.20: Comparison of Common Mode (CM) in Time and Frequency approach.

Table 3.2: Computation Time between Frequency Domain simulation and Time Domain simulation - Low Voltage Buck Converter

	Frequency Domain Modeling	Time Domain Modeling
Calculation Time	0.412s	106.854s

3.2 Modeling a High Voltage Buck Converter

3.2.1 Discontinuous conduction Time Domain Modeling

Time Domain structure in Discontinuous Conduction Mode

In the same vein, the subsequent modeling was performed on a Buck converter operating in Discontinuous Conduction Mode (DCM). Despite the limited resources available for modeling in discontinuous conduction, the goal was to apply the same methodology used for continuous conduction. Figure 3.21 illustrates the time domain structure of a Buck converter simulated in LTspice operating in DCM.

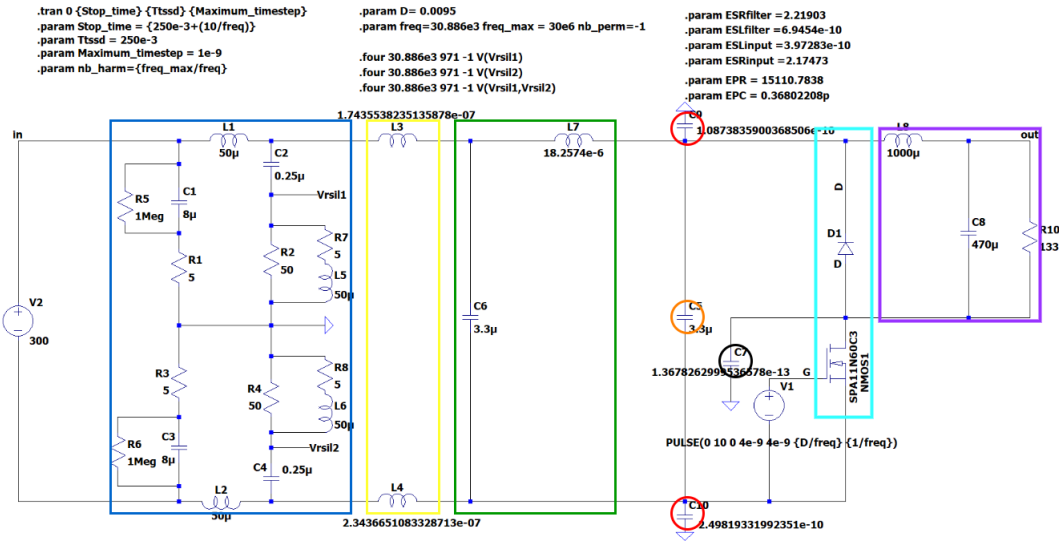


Figure 3.21: Time domain Structure of a High Voltage Buck Converter in Discontinuous Conduction Mode.

This step enabled us to understand the behavior of a buck converter in discontinuous conduction, as well as the influence of various components. This approach complements the results measured with the EMSCOPE device. The structure in Figure 3.21 accounts for the parasitic elements of each component, which are detailed in Table 3.3 along with their respective descriptions.

Extraction of the disturbance spectrum from Time Domain simulation

Table 3.3: Parameters of Marked Components

Component	Characteristic
LISN	The simplified structure of the LISN.
L3, L4	Represents a cable between the LISN and the power converter with $1\mu\text{H}/\text{m}$ of cable
C6	Represents the capacitance of the Filter $=3.3\mu\text{F}$ with ESR= 2.219Ω , ESL= 0.694nH .
L7	Represents the Inductance of the Filter
C5	Input capacitor of $3.3\mu\text{F}$ with ESR= 2.17473Ω , ESL= 0.397nH .
Zmc	A common-mode impedance= 0.13678pF , that models the impedance between the ground plane of the converter and that of the EMSCOPE setup.
MOSFET	NMOS transistor IPF039N03L that acts as a switch for the buck converter topology.
D4	Represents an ideal freewheeling diode.
L8	Output inductance of $1000\mu\text{H}$
C8	$470\mu\text{F}$ output capacitor of the LC filter with ESR= $1\text{m}\Omega$
Rload	Output ideal resistor $=133\Omega$ to reach the operating point of the prototype.

In Figure 3.21, it can be noted that the `.four` function in LTspice was used on the VLISN1 (Phase), VLISN2 (Neutral), and Differential Mode voltages to obtain the spectrum of multiple harmonics of the switching frequency (30.886 kHz). The use of this function allows for the determination of the amplitudes of these harmonics, which are the only frequencies capable of carrying energy and thus contributing to conducted disturbances.

Consequently, the obtained spectrum is consistent over the frequency range specified by the conducted disturbance standards. Figures 3.22, 3.23, and 3.24 show the spectrum obtained from VLISN1, VLISN2, and Differential Mode voltage.

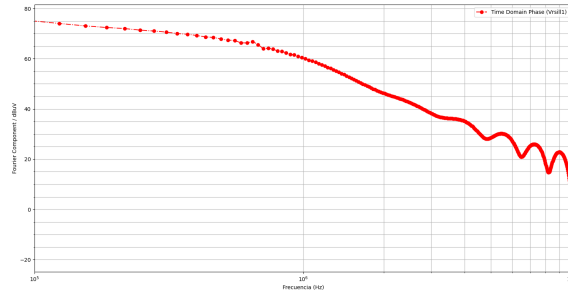


Figure 3.22: Perturbation spectrum extracted with the function ".four" in Discontinuous conduction of VLISN1 (Phase).

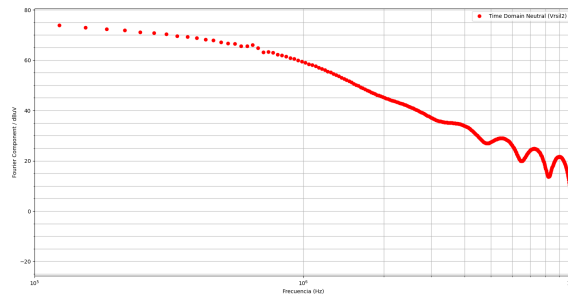


Figure 3.23: Perturbation spectrum extracted with the function ".four" in Discontinuous conduction of VLISN2 (Neutral).

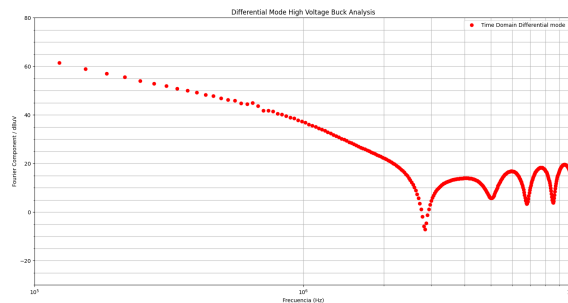


Figure 3.24: Perturbation spectrum extracted with the function ".four" in Discontinuous conduction of Differential Mode Voltage (DM).

For the Common Mode voltage analysis, a different method is employed due to the absence of suitable nodes in LTspice for the `.four` analysis. Instead, the program's FFT function is used, where $\frac{VLISN1+VLISN2}{2}$ is calculated. The obtained spectrum is converted to `.txt` format and its information is post-processed to obtain the Common Mode values, shows in Figure 3.25.

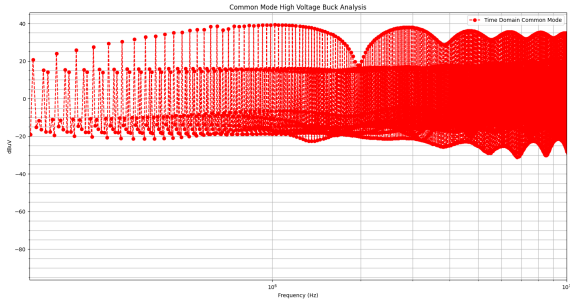


Figure 3.25: Perturbation spectrum extracted with the function `'.txt'` in discontinuous conduction of Common Mode Voltage (CM).

3.2.2 Discontinuous conduction Frequency Domain modeling

As mentioned earlier, to perform frequency domain modeling, two criteria are needed:

1. **Identification and linearization of disturbance sources.**
2. **Identification of propagation paths.**

The objective is to be able to achieve the frequency structure presented in Figure 3.26.

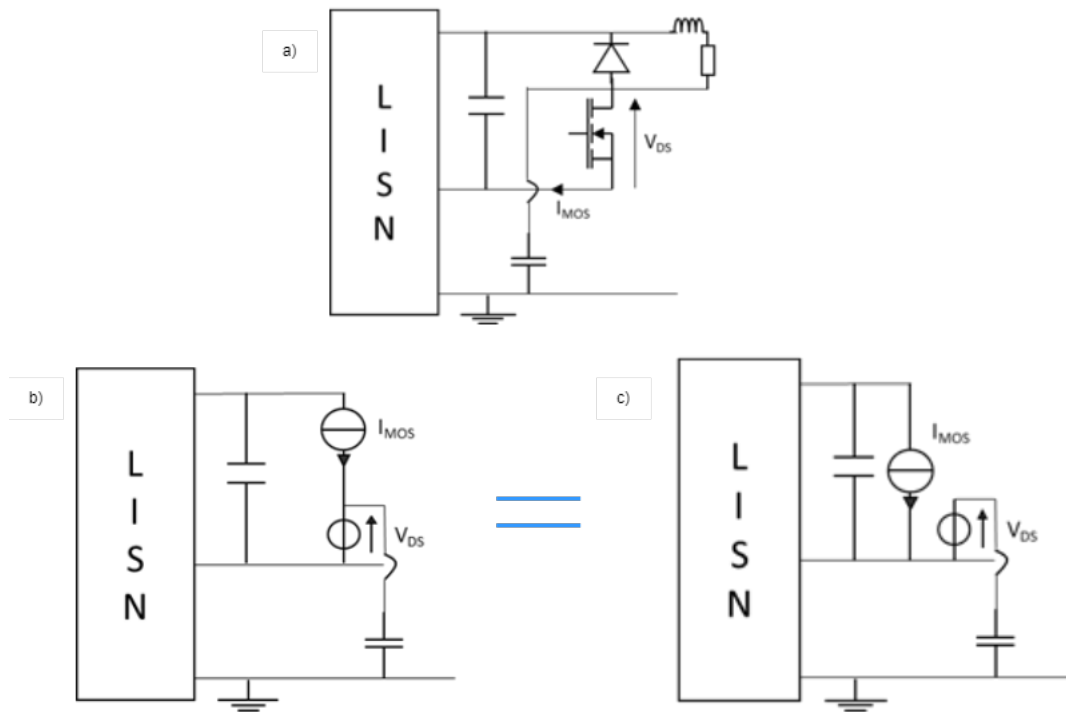


Figure 3.26: a. Diagram of the time domain representation b. First configuration of Frequency domain structure c. Second configuration of frequency Domain structure.

Modeling of disturbance sources

The methodology used here is the same as that previously employed in the modeling of the low voltage buck converter. We will only highlight the crucial differences in the configuration for high voltage.

One big change appears in the formulation on the equations in the Laplace domain. This domain was chosen because it remains simple to implement under LTspice. This allowed us to arrive at equations 3.3 and 3.4.

Equation 3.3: Laplace transform of I_{DS} following a triangular approximation.

$$I_{\text{MOS}}(s) = 2 \cdot f_{\text{sw}} \left[\frac{I_{\text{pk}}}{(d \cdot T_{\text{sw}} - t_{\text{fi}}) \cdot s^2} \cdot \left(1 - e^{-s \cdot (d \cdot T_{\text{sw}} - t_{\text{fi}})} \right) - e^{-s \cdot (d \cdot T_{\text{sw}} - t_{\text{fi}})} \cdot \frac{I_{\text{pk}}}{t_{\text{fi}} \cdot s^2} \cdot \left(1 - e^{-s \cdot t_{\text{fi}}} \right) \right] \quad (3.3)$$

- $I_{\text{MOS}}(s)$: Represents the current through the MOSFET as a function of the complex frequency variable s in the Laplace transform domain.
- s : The Laplace transform variable representing complex frequency, used to analyze systems in the frequency domain.
- f_{sw} : The switching frequency of the device or circuit. This frequency indicates how often the MOSFET is turned on and off per unit of time and is crucial in determining the response time and efficiency of power converters.
- I_{pk} : The peak current, likely representing the maximum current that flows through the MOSFET during its operation cycle.
- d : The duty cycle, which is the fraction of the total period during which the MOSFET is conducting. It significantly affects the average output in power electronic applications.
- T_{sw} : The total switching period, representing the time for one complete on/off cycle of the MOSFET $1/(f_{\text{sw}})$.
- t_{fi} : The fall time, indicating the duration over which the current or voltage falls from a higher to a lower value (or zero). This time is critical in determining the speed at which the MOSFET can stop conducting.

Equation 3.4: Laplace transform of V_{ds} following a trapezoidal approximation.

$$V_{DS}(s) = 2 \cdot f_{\text{sw}} \left[\frac{-V_{dc}}{t_{fv} \cdot s^2} \cdot \left(1 - e^{-s \cdot t_{fv}} \right) + e^{-s \cdot (d \cdot T_{\text{sw}} - t_{fi} - t_{rv})} \cdot \frac{V_{dc}}{t_{rv} \cdot s^2} \cdot \left(1 - e^{-s \cdot t_{rv}} \right) - e^{-s \cdot (d + \beta) \cdot T_{\text{sw}}} \cdot \frac{A \cdot \omega}{\omega^2 + s^2} \right] \quad (3.4)$$

- $V_{DS}(s)$: The drain-to-source voltage of the MOSFET as a function of s , represented in the Laplace transform domain, indicating how the voltage responds over time in the frequency domain.
- s : The Laplace transform variable representing complex frequency, used to analyze systems in the frequency domain.

- f_{sw} : The switching frequency of the MOSFET, which affects how often the MOSFET turns on and off, influencing the efficiency and operation of the circuit.
- V_{dc} : The DC voltage applied across the MOSFET, which is a primary factor in determining the operation and power level of the device.
- t_{fv} : Fall time of voltage, the duration it takes for the voltage to decrease from a high value to a low value or zero during each cycle.
- t_{rv} : Recovery time voltage, the time required for the voltage to recover or return to a normal state after a transient or interruption.
- d : Duty cycle of the MOSFET, which describes the fraction of one complete cycle during which the MOSFET is active.
- T_{sw} : The total switching period, representing the time for one complete on/off cycle of the MOSFET $1/(f_{sw})$.
- t_{fi} : Fall time of the current, the time taken for the current to fall from a specified level to zero or a lower level during the switching process.
- β : A parameter possibly modifying the duty cycle or other temporal characteristics in the circuit, reflecting phase shifts or adjustments in timing.
- A : Represents an amplitude or scaling factor in a term that might describe a resonant or oscillatory component in the circuit.
- ω : The angular frequency related to the oscillatory or resonant components of the circuit, involved in defining the response characteristics at specific frequencies.

The trapezoidal and triangular approximation does not take into account the high-frequency oscillations at the opening and closing of the NMOS. The advantage of this approximation, however, is its simple description of the behavior of the converter, thus allowing an estimate of the real spectrum. Let us consider the generic equation of the Laplace transform of trapezoidal shape for voltage and triangular shape for current, as shown in Figure 3.27:

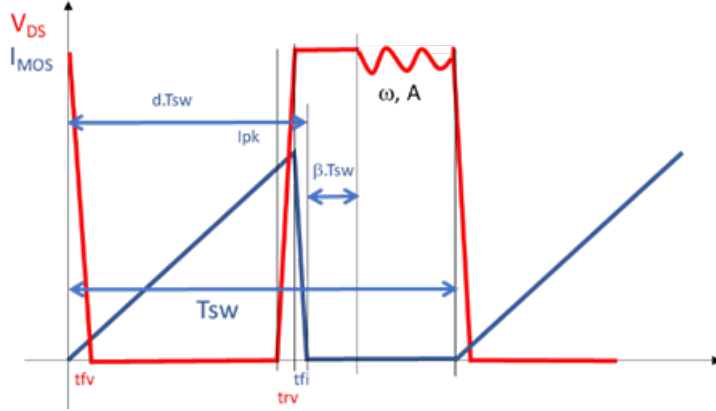


Figure 3.27: Time domain representation of $V_{DS}(t)$ and $I_{MOS}(t)$ used in the Laplace transform expressions (DCM).

Implementing the Frequency Domain Structure in LTSpice

The sources of disturbances for frequency domain modeling are represented by equivalent voltage and current generators, defined using Laplace equations. This approach enables linearization and direct simulation in the frequency domain with LTSpice. For a buck converter with a single switching cell, the disturbances are modeled as I_{ds} and V_{ds} , corresponding to the current flowing through and the voltage across the NMOS switch, respectively. To implement these equations in LTspice, voltage controlled voltage source (E1) and voltage controlled current sources (G1) are used, as illustrated in Figure 3.28. These generators, controlled by Laplace equations, correspond to the MOSFET drain current (equation 3.3) and drain-to-source voltage (equation 3.4), and are excited by a 1V AC voltage for frequency simulation [10].

The implementation of Laplace sources and equations has been validated through previous work [2], demonstrating that LTspice can effectively simulate frequency structures using linearized equivalent generators. The key advantage of using LTspice for frequency domain modeling is the intuitive definition of propagation paths by arranging disturbance sources in series or parallel, eliminating the need for complex analytical calculations of propagation paths. This approach significantly saves time compared to purely analytical frequency domain modeling, which involves intricate transfer function calculations to model the overall impedance affecting the disturbance sources [9].

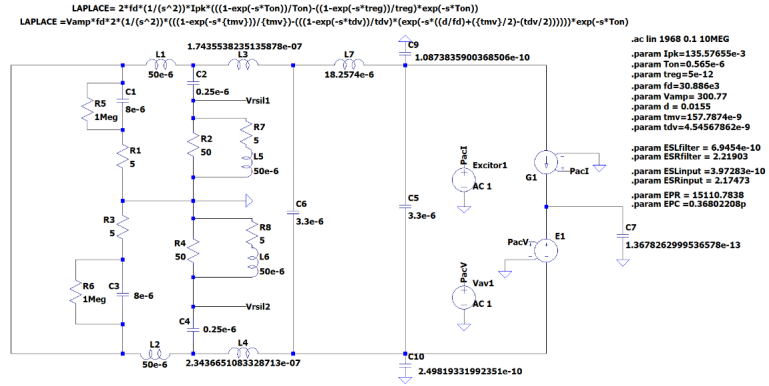


Figure 3.28: Simulated Frequency Domain structure of a buck converter in Discontinuous conduction Mode.

Extraction of the disturbance spectrum Frequency Domain

The frequency domain analysis begins with setting up and simulating the circuit in LTspice, ensuring that each component is accurately placed according to the provided schematic. A linear frequency sweep analysis is performed from 0 Hz to 10 MHz to obtain a comprehensive representation of the entire spectrum. This data will later be compared with the measured data from the prototype in Chapter 4. The output of this simulation is saved in a .raw file.

Following the simulation, the data is extracted and processed using a specialized script, with a focus on the voltage traces of the relevant nodes. These voltage values are then converted into decibel microvolts (dB μ V) for clarity and ease of analysis. The subsequent steps involve plotting the frequency response for critical nodes, including Differential Mode and Common Mode, as illustrated in Figures 3.29 and 3.30.

In this buck converter, we will only consider the differential mode voltage and the common mode voltage, as they are the most critical factors for filter modeling. Since we are not taking all elements into account, there is a trade-off effect between the differential mode and the VLISN1, VLISN2 voltages. This trade-off prevents a perfect alignment of the three voltages.

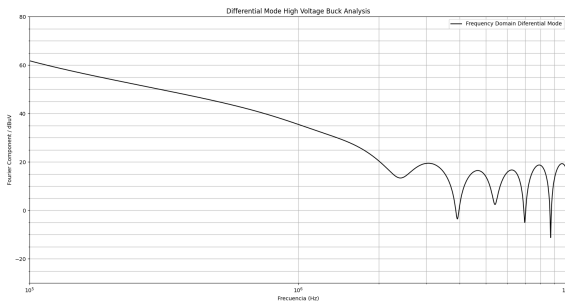


Figure 3.29: Comparison of Differential Mode(DM) - Time domain Mode vs Frequency Domain.

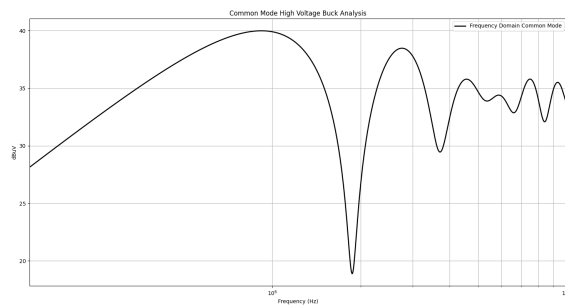


Figure 3.30: Comparison of Common Mode (CM) - Time domain Mode vs Frequency Domain.

3.2.3 Comparison of the results of discontinuous conduction simulations

Before comparing the perturbation spectra, it is crucial to validate the correct implementation of the equivalent generators. If significant differences are identified, as shown in Figures 3.31 and 3.32, it is likely that the two models are not operating under the same conditions. Therefore, it is important to check and confirm the values of the various parameters used in the frequency modeling.

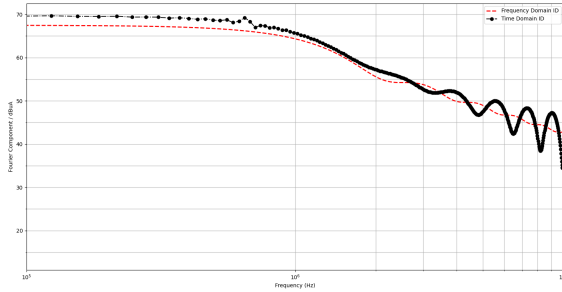


Figure 3.31: Comparison of Source ID - Time domain Mode vs Frequency Domain.

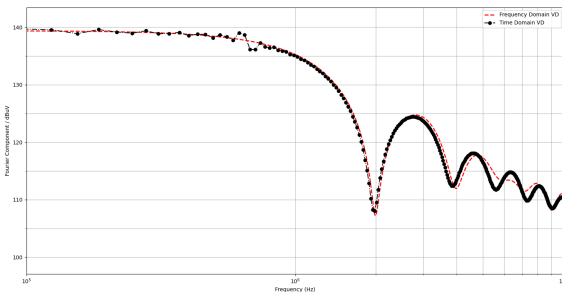


Figure 3.32: Comparison of Source VD - Time domain Mode vs Frequency Domain.

The advantage of frequency domain modeling is highlighted through very short simulation in comparison with the time domain as shows in the Table 3.4. Indeed, with very low computation times, frequency domain modeling is a suitable tool for optimizing an EMC filter like in the figures 3.33 and 3.34.

Table 3.4: Computation Time between Frequency Domain simulation and Time Domain simulation - High Voltage Buck Converter

	Frequency Domain Modeling	Time Domain Modeling
Calculation Time	0.512s	4006.854s

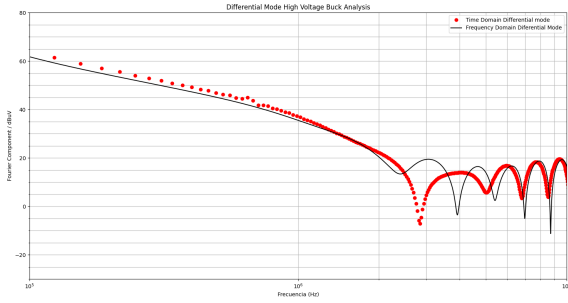


Figure 3.33: Comparison of Differential Mode(DM) - Time domain Mode vs Frequency Domain.

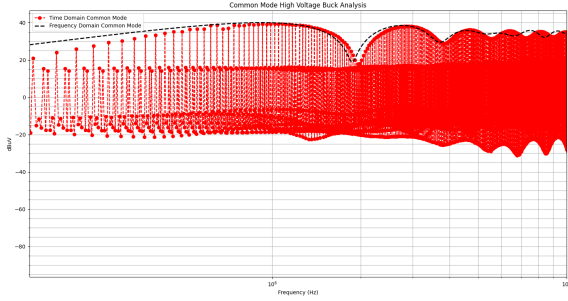


Figure 3.34: Comparison of Common Mode (CM) - Time domain Mode vs Frequency Domain.

3.3 Modeling a Double Buck Converter

3.3.1 Time Domain Modeling

The double Buck converter design includes two stages as shows in figure 3.35, a high-voltage stage (RED) operating in discontinuous conduction mode (DCM) and a low-voltage stage (BLUE) operating in continuous conduction mode (CCM). This dual-stage approach optimizes the converter's efficiency under varying load and voltage conditions [11].

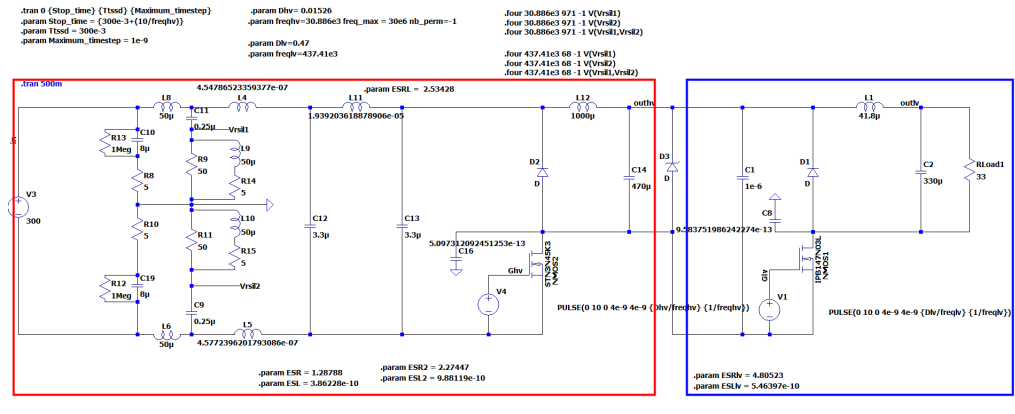


Figure 3.35: Time domain Modeling of the double buck converter structure.

Structure in Time Domain

In Figure 3.35, it can be noted that the '.four' function of LTspice is used for FFT calculations to visualize the present harmonics. Since this function operates at a specific frequency, in this double buck converter configuration, the predominant frequency is that of the initial buck converter. In this case, it is the high-voltage buck converter (RED). Considering this, we know that the switching frequency is 30.886 KHz.

Thus, the spectrum obtained is consistent over the frequency range of interest (150 KHz - 10 MHz) [1].

Extraction of the waves in Time Domain

In the following figure 3.36, we can observe the extraction of the Fourier components 'four' of the mentioned structure especially of the Differential Mode voltage.

A different method is used for obtaining the Common Mode since we do not have any nodes provided by LTspice to apply the ".Four" analysis.

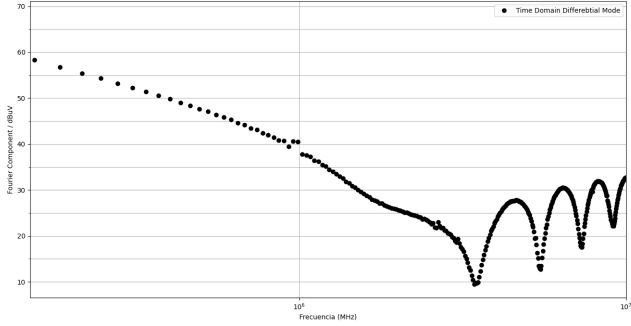


Figure 3.36: Time domain spectrum of double buck Differential Mode (DM).

We use the program's "FFT" function where we calculate $\frac{VLISN1+VLISN2}{2}$. The obtained spectrum is converted to .txt format and its information is post-processed to obtain the Common Mode values, shown in Figure 3.37.

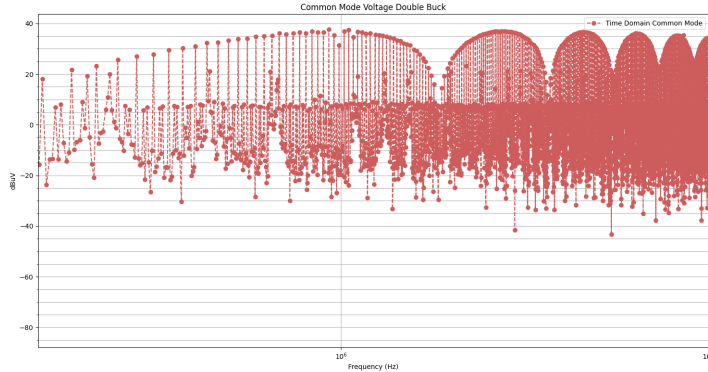


Figure 3.37: Time domain spectrum of double buck Common Mode (CM).

3.3.2 Frequency Domain Modeling

The methodology used here in figure 3.38, is the same as that previously employed in the modeling of the low voltage buck converter and the high voltage. We will only highlight the crucial differences in the configuration for Double Buck Configuration.

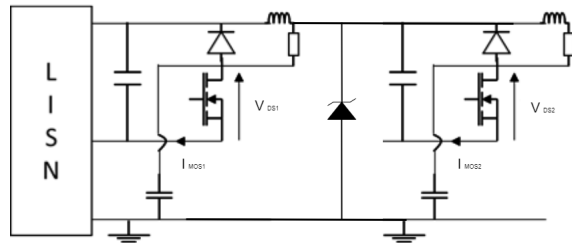


Figure 3.38: Diagram of the time domain representation.

Structure in frequency Domain

In the structure of the double buck converter we can delimit the 2 previous structures mentioned above united in a single scheme as shown in figure 3.39, where the section delimited by the blue squares belong to the high voltage stage and the sections enclosed by the orange squares determine the low voltage stage.

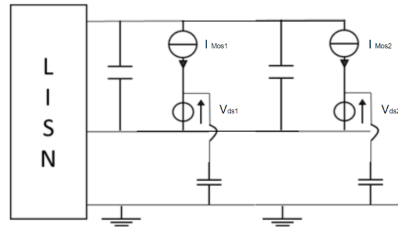


Figure 3.39: Diagram of the Frequency domain representation.

Extraction of the waves in Frequency Domain

The frequency domain analysis begins with the setup and simulation of the circuit using LTspice, as shown in the figure 3.40, where each component is accurately placed according to the schematic provided.

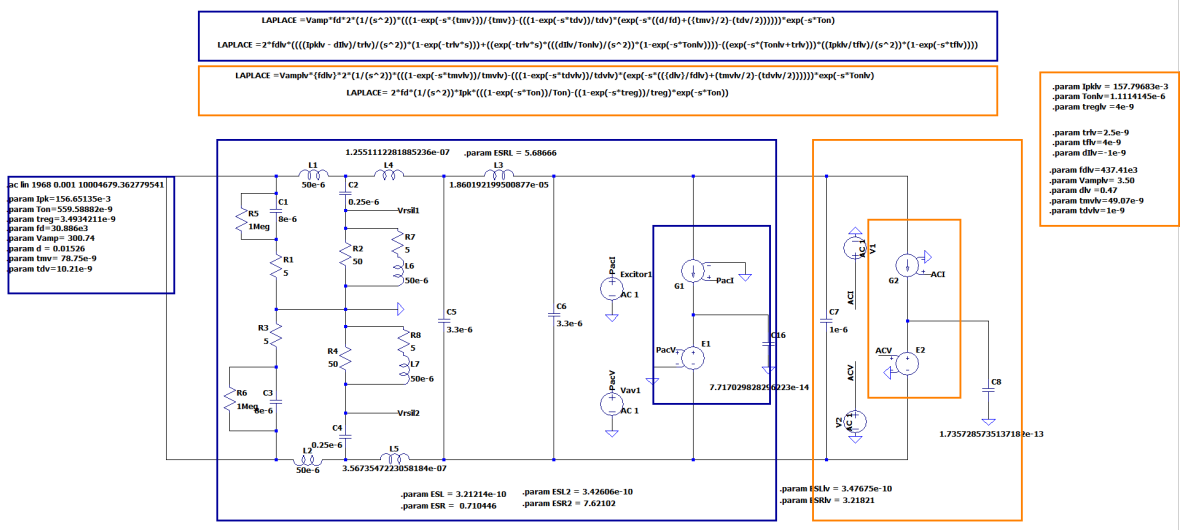


Figure 3.40: Diagram of the Frequency domain representation.

Perform a frequency sweep analysis from 150 KHz to 10 MHz and save the output in a .raw file. After simulation, extract and process data from this file using a specialized script, focusing on extracting voltage traces of the interest nodes. These voltage values are then converted into decibels micro volts for clarity and ease of analysis. In the figures 3.41 and 3.42 they show the subsequent steps involve plotting the frequency response for critical nodes including Differential Mode and Common Mode respectively.

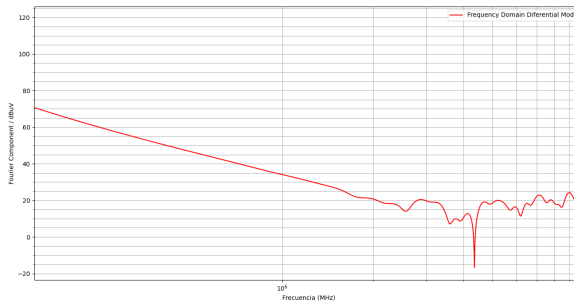


Figure 3.41: Extraction of the waves of differential Mode in Frequency Domain.

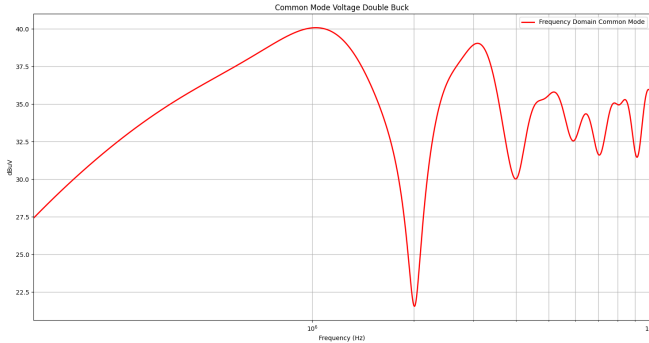


Figure 3.42: Extraction of the waves of Common Mode in Frequency Domain.

3.3.3 Comparison of the simulations results

Before comparing the perturbation spectra, it is essential to validate the correct implementation of the equivalent generators. If significant differences are identified, as shown in Figures 3.43 and 3.44, it is likely that the two models are not operating under the same conditions. Therefore, it is important to verify and confirm the values of the various parameters used in the frequency modeling [11].

In this buck converter we have the same effect like the high voltage buck so, we will only consider the differential mode voltage and the common mode voltage, as they are the most critical factors for filter modeling. Therefore, only the differential mode and common mode are considered, as they are the prioritized data in the modeling process.

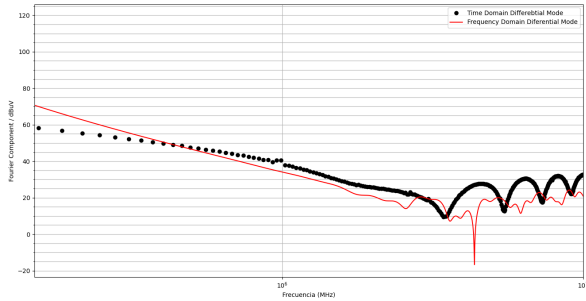


Figure 3.43: spectrum of the Frequency domain vs Time domain voltages of Differential Mode.

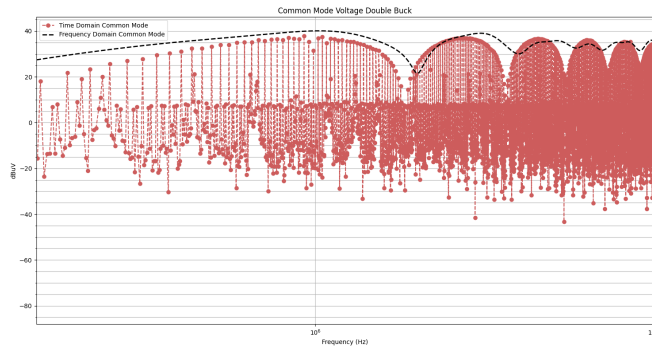


Figure 3.44: spectrum of the Frequency domain vs Time domain voltage of Common mode.

The advantage of frequency domain against time domain modeling is highlighted through very short simulation times shows in the Table 3.5.

Table 3.5: Computation Time between Frequency Domain simulation and Time Domain simulation - Double Buck Converter

	Frequency Domain Modeling	Time Domain Modeling
Calculation Time	0.512s	27006.854s

Chapter 4

Modeling methodology validation

4.1 Experimental phase-perturbation measurement

In order to validate the use of frequency domain modeling to estimate the spectrum of conducted disturbances, an experimental phase was carried out. The objective of this phase is to compare these simulation results obtained in Chapter 3. The measurements were carried out using the EMSCOPE device, where they were compared with the prototypes developed on a low-voltage buck converter board, a high-voltage buck converter, and finally a model of a double buck that combines a high-voltage buck and a low-voltage buck. A waveform study conducted in Chapter 3 was used for the construction of the models in both the time domain and the frequency domain.

4.2 Comparison of Results

In order to confirm the use of frequency domain modeling for the estimation of conducted disturbance spectra, the simulation results of a high voltage buck converter, a low voltage buck converter and a double buck converter, the first two in continuous and discontinuous conduction respectively, were compared with the measurement results.

4.2.1 Low voltage Buck configuration

Figure 4.1 shows the EMSCOPE device, which is used to field the voltage spectrum of both differential mode and common mode, this spectra are shown in Figure 4.2 and 4.3 in blue where it compares with the simulations previously performed in Chapter 3.



Figure 4.1: Generation of the measure data with EMSCOPE and connection of low voltage buck converter.

In the figure 4.2, the blue line represents the measured harmonic components of the differential mode across the frequency spectrum. The red curve corresponds to the frequency domain spectrum, while the black points show the spectrum in the time domain. The agreement between the simulated (red and black) and measured (blue) data validates the proposed model in the theoretical analysis within the frequency range of interest.

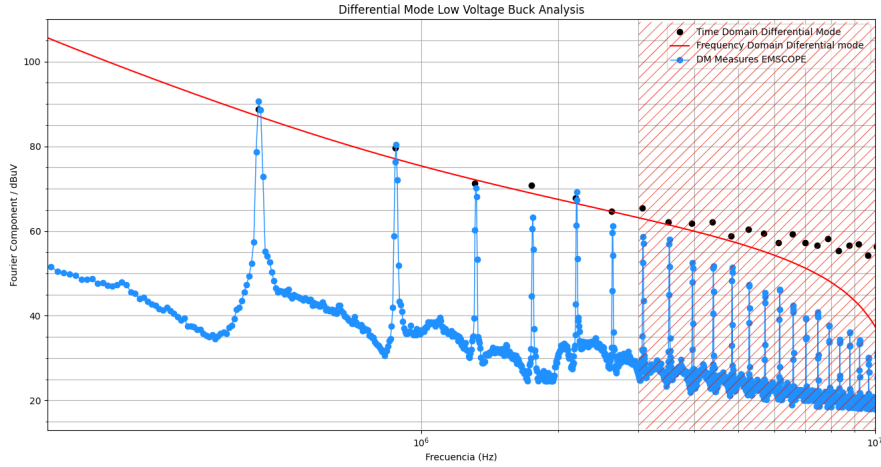


Figure 4.2: Diagram of the Frequency domain representation with measurement data

In the figure 4.3, the blue line represents the measured harmonic components of the Common mode across the frequency spectrum. The red curve corresponds to the frequency domain spectrum, while the black points show the spectrum in the time domain. The agreement between the simulated (red and black) and measured (blue) data validates the proposed model in the theoretical analysis.

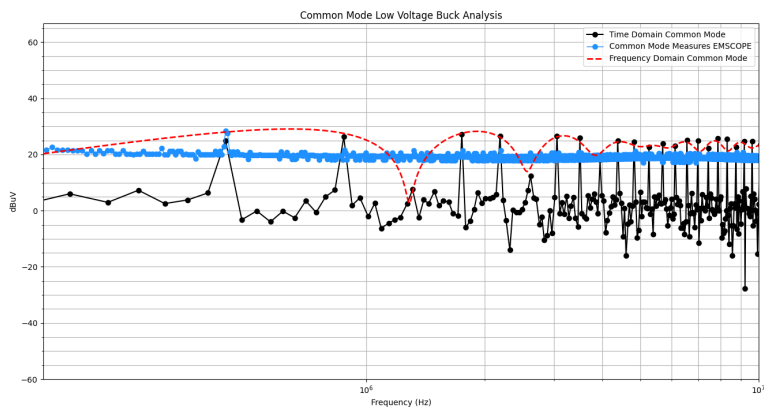


Figure 4.3: Diagram of the Frequency domain representation with measurement data.

The differences observed between the measurement and simulation, especially at higher frequencies, could be attributed to unmodeled effects in the analysis or limitations of the measure-

ment instruments. Nonetheless, the results generally show good agreement, thereby validating the approach used to model the electromagnetic interference characteristics of the low voltage Buck converter .

4.2.2 High voltage Buck configuration

Figure 4.4 shows the EMSCOPE device, which is used to field the voltage spectrum of both differential mode and common mode, this spectrum is shown in Figure 4.5 and 4.6 in blue where it compares with the simulations previously performed in Chapter 3.

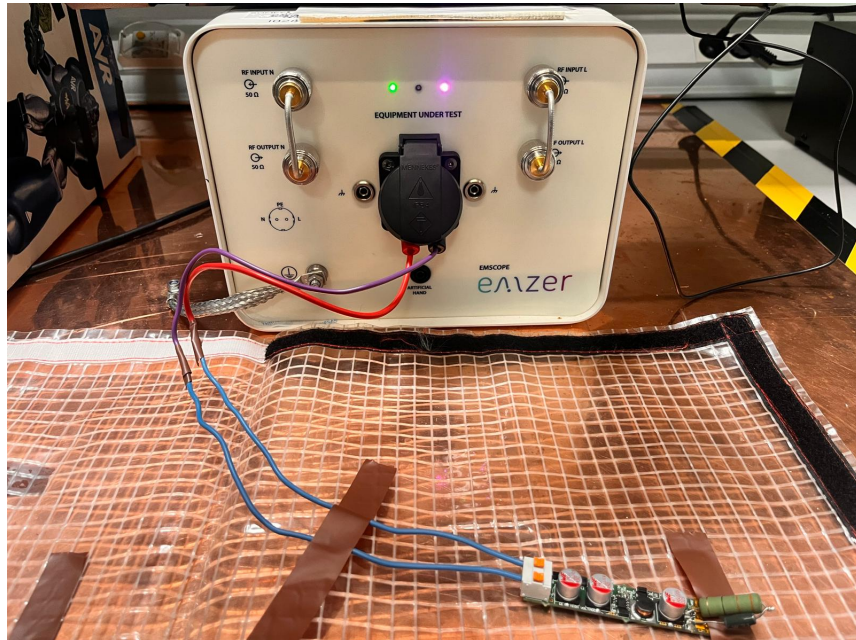


Figure 4.4: Generation of the measure data with EMSCOPE and connection of high voltage buck converter

Figure 4.5 and 4.6 shows the analysis of the differential mode and common mode in a high-voltage Buck converter using the EMSCOPE device. The blue line represents the measured voltage spectrum, while the black curve shows the frequency domain spectrum, and the red points represent the time domain spectrum.

The close alignment between the measured (blue) and simulated (red and black) data sup-

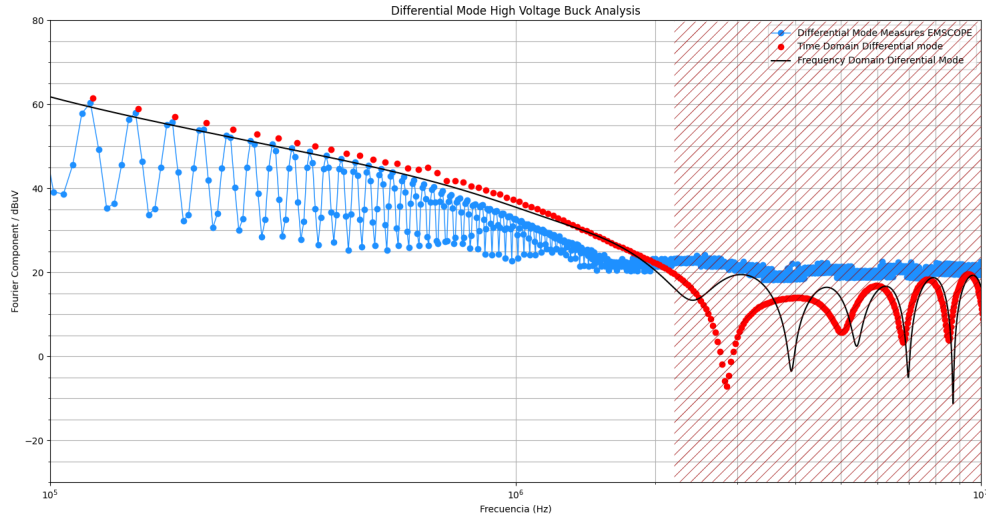


Figure 4.5: Diagram of the Frequency domain representation with measurement data.

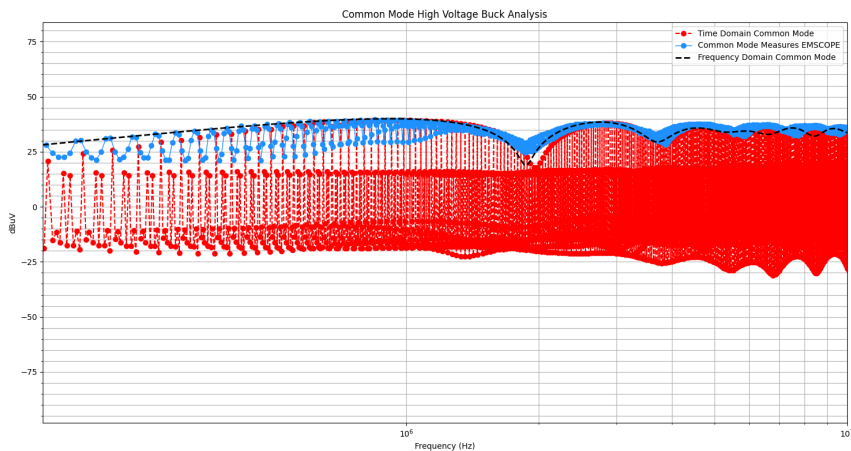


Figure 4.6: Diagram of the Frequency domain representation with measurement data.

ports the accuracy of the theoretical model. Minor discrepancies at higher frequencies may be due to unmodeled effects or measurement limitations, but overall, the results confirm the validity of the electromagnetic interference analysis of the high voltage Buck converter.

4.2.3 Double Buck configuration

Figure 4.7 shows the EMSCOPE device, which is used to field the voltage spectrum of both differential mode and common mode, this spectra are shown in Figure 4.8 and 4.9 in blue where it compares with the simulations previously performed in Chapter 3.

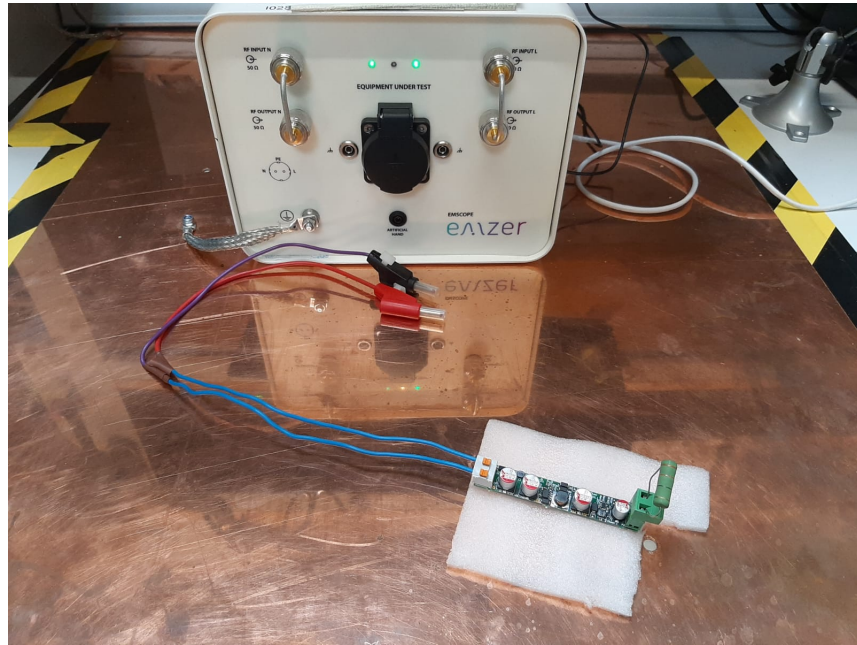


Figure 4.7: Generation of the measure data with EMSCOPE and connection of double buck converter.

Figures 4.8 and 4.9 shows the analysis of the differential mode and Common mode in a double Buck converter using the EMSCOPE device. The blue line represents the measured voltage spectrum, while the red curve shows the frequency domain spectrum, and the black points represent the time domain spectrum.

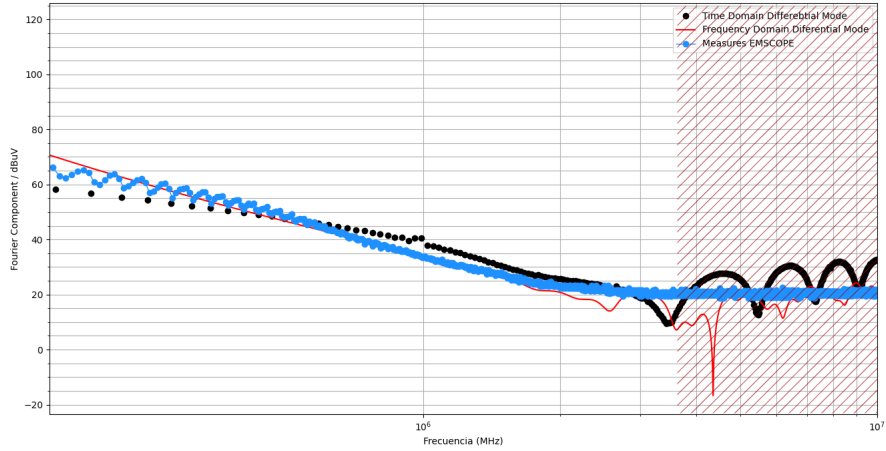


Figure 4.8: Diagram of the Frequency domain representation with measurement data.

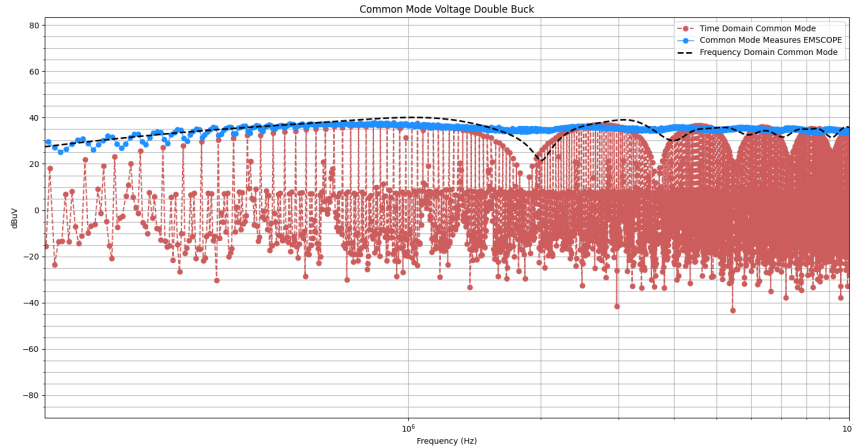


Figure 4.9: Diagram of the Frequency domain representation with measurement data.

The strong correlation between the measured (blue) and simulated (red and black) data confirms the accuracy of the theoretical model. Although there are slight discrepancies at higher frequencies, possibly due to unmodeled effects or measurement limitations, the overall results validate the electromagnetic interference analysis for the differential mode in the double Buck converter.

The failure to take into account all these elements could explain the differences observed

between 3MHz and 10MHz. However, the results of the frequency domain modeling in black agree well with the time domain modeling in red. Comparison with the measurement (blue) in Figures 4.2, 4.5 and 4.8 shows that the estimation up to 3 MHz works correctly. Therefore, by making the model more complex to account for additional elements, it is very likely to increase the validity domain of the estimation by frequency domain modeling.

Chapter 5

Automatizing and Optimization circuit Process

5.1 Automatizing

The frequency domain modeling could make some users scary. Indeed, the use of the Laplace equations could be considered as too much complicated and therefore prohibitive. To prevent this, one goal of my internship was to develop an automatic tool. Its goal is to help the people using easily frequency domain modeling for switch mode power supplies instead of the well known time domain modeling.

For the automation process, an open-source environment was developed due to its greater reach and adaptability. The choice for this mission was Python, as it provides immense versatility when analyzing data from LTspice, thanks to libraries that work directly with LTspice looks in the figure 5.1. The features of the tool will be shared in the upcoming paragraph.

- **Initial Configuration:** First, the script establishes the path to LTspice, which must be provided as an argument when running the script from the command line. This ensures that the system can locate and execute LTspice for the simulation.
- **Preparation for Simulation:** The user specifies the schematic or netlist file to be simulated. The script constructs and executes a command that involves LTspice in batch processing mode, allowing the simulation to be performed without manual intervention and directly from the

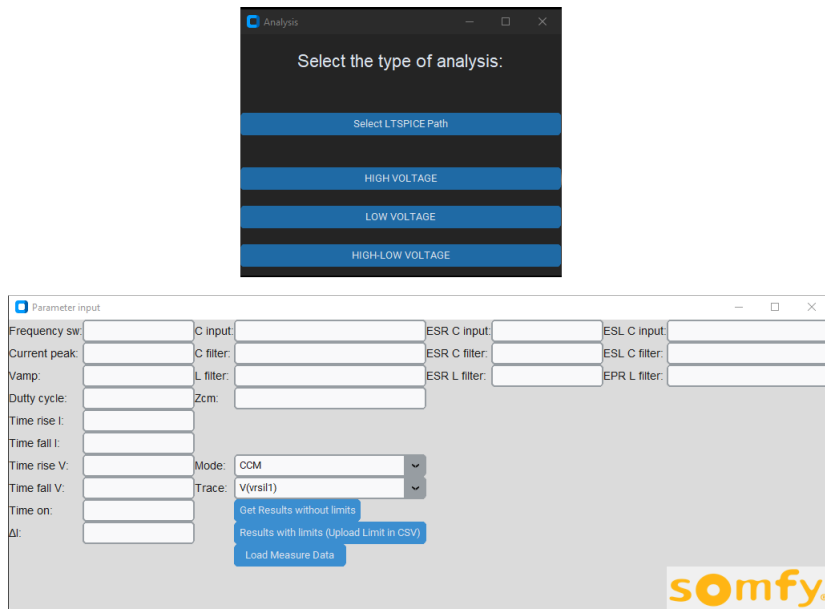


Figure 5.1: Automatizing tool for circuit analysis in frequency domain

script.

- **User Interface:** A graphical interface developed with customtkinter is used, allowing the user to input specific parameters that will influence the simulation. These parameters may include switching frequency, current peaks, voltage amplitude, among others.
- **Dynamic Netlist Editing:** Before executing the simulation, the script dynamically modifies the netlist according to the parameters entered by the user. This is done using the SpiceEditor class from PyLTSpice, allowing precise customization of components such as voltage and current sources, as well as other passive and active elements as needed.
- **Simulation Execution:** Once the netlist is configured, the script re-executes LTspice with the modified file. The simulation result is checked, and the user is notified whether it was completed successfully or if there were errors.
- **Result Analysis:** The simulation results are read using the RawRead class from PyLTSpice, which allows extracting specific data such as voltages and currents at different points in the circuit. Various graphical visualizations based on these data are offered, allowing the

user to analyze components in the frequency domain or compare standard and simulated measurements.

- **Interaction and Visualization:** The graphical interface also allows loading real measurement data from CSV files to compare them with the simulated results. Additionally, it provides interactive tools to adjust visualizations and better understand the circuit behavior under different operating conditions.

This approach not only automates circuit simulation and analysis but also provides a powerful and flexible tool for designers and engineers, facilitating experimentation and optimization of electronic circuits in a controlled and accessible environment.

5.2 Optimization

To be able to have better match between simulation results and measurement data, an optimization approach was developed. The circuit optimization process used in this methodology follows a structured approach to adjust the parameters of the circuit components (Dynamic netlist) and minimize discrepancies between simulated results and real-world measured data. The methodology employed is described below, as shown in the figure 5.2:

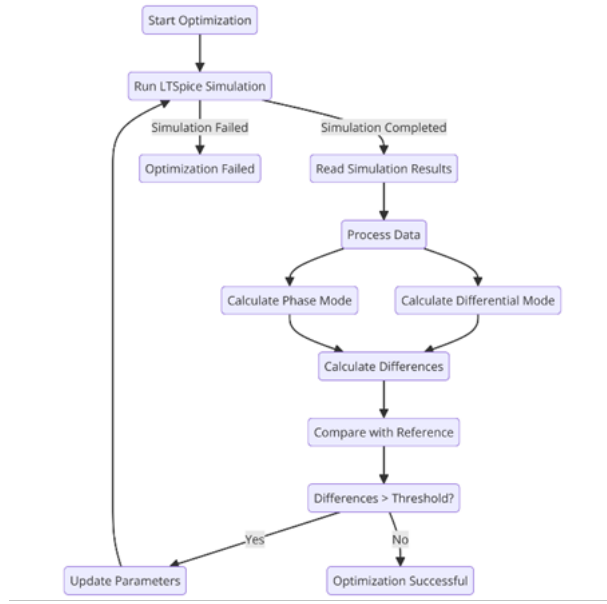


Figure 5.2: Optimization process to identify all stray elements. The EMC frequency models are included into an optimization loop to identify the model parameters, thanks to a comparison between measured and conducted EMI

- **Circuit Initialization and Simulation:** The process begins with a predefined electrical circuit, whose behavior is simulated to obtain specific response values, such as signal magnitudes at different frequencies.
- **Result Analysis:** The simulation results are compared with reference data obtained from real measurements. This comparison is conducted at specific points in the frequency spectrum, identifying differences between the simulated and measured magnitudes.
- **Error Identification:** If the differences between the simulated and measured magnitudes exceed a predefined threshold, the circuit model is considered to be inadequately adjusted. At this point, the components responsible for these discrepancies are identified.
- **Parameter Adjustment:** The parameters of the circuit components (such as resistances, inductances, and capacitances) are randomly adjusted within a reasonable range. This adjustment aims to modify the circuit's response so that the differences with real data are reduced.

- **Iteration:** The process of simulation, result analysis, and parameter adjustment is repeated iteratively. In each iteration, the new component values are tested, and the results are again compared with the real measurements. The goal is that with each iteration, the discrepancies are minimized.
- **Convergence:** The iteration process continues until the differences between the simulated values and real measurements are sufficiently small, indicating that an optimal circuit configuration has been reached.
- **Validation:** Finally, once the differences are within an acceptable range, the results are validated to ensure that the optimized circuit meets the desired requirements and specifications.

In the figure 5.3 and 5.4, the impact of the optimization process in Differential Mode Voltage of a Low voltage buck converter, is illustrated. After executing the process, values for the components are obtained that align well with the analyzed prototype.

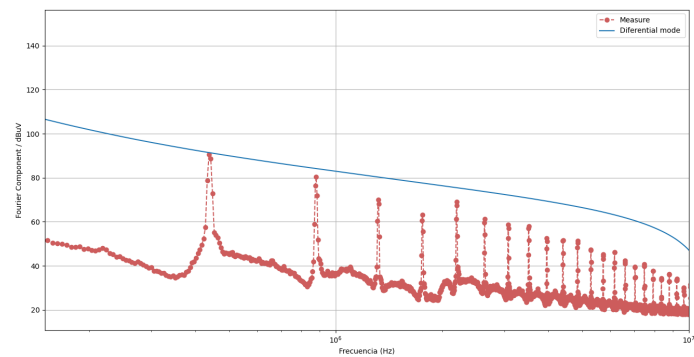


Figure 5.3: Result before the optimizing process

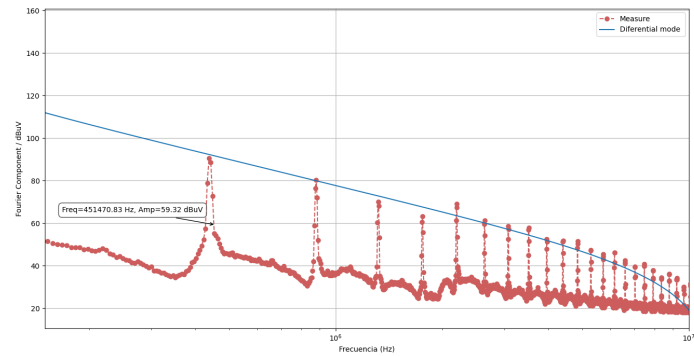


Figure 5.4: Result after the optimizing process

Chapter 6

Conclusions

This study has presented a robust methodology for the estimation and modeling of electromagnetic interference conducted in switched-mode power supplies. Through the implementation of models in the time and frequency domains and their validation with experimental tests using the EMSCOPE device, we have demonstrated that frequency domain modeling is an effective and efficient tool to anticipate and mitigate conducted disturbances, facilitating the preliminary design of EMC filters.

The obtained results not only validate the accuracy of the proposed models compared to experimental approaches, but also highlight the usefulness of LTspice software for fast and accurate simulation of these complex phenomena. This research provides a solid foundation for future developments in the design of more efficient power converters that are less susceptible to electromagnetic interference.

However, we recognize some inherent limitations of our approach, such as the reliance on linear assumptions and the idealization of certain switching conditions that may not be fully representative of real operating scenarios. These limitations suggest the need for future research to explore more inclusive models that consider more complex nonlinear and dynamic behaviors.

Chapter 7

Recommendations and prospects

The following recommendations are proposed based on the insights gained during the internship:

1. **Expansion of Simulation Models:** Integration of non-linear effects and transient behavior in simulation models is recommended. This could be achieved through the development of additional modules in LTspice or by using alternative simulation software that offers greater flexibility to model complex dynamics and transients.
2. **Enhanced Experimental Validation:** To ensure the applicability of the models under a wider range of operational conditions, it is essential to expand experimental validation. This would include testing under different load configurations and with variations in temperature and other environmental factors.
3. **Development of EMC Filter Prototypes:** Based on the results obtained, it is suggested to design and manufacture optimized EMC filter prototypes. These filters should be evaluated in real environments to measure their effectiveness in reducing electromagnetic interference in industrial and commercial applications.
4. **Training and Education:** Implement training programs for electronic and power system designers, focused on advanced modeling and simulation techniques for EMC. This will help bridge the gap between theory and practice, equipping professionals with the necessary skills to face emerging challenges in the field.
5. **Interdisciplinary Collaboration:** Establish collaborations between academics, industry engineers, and electronic component manufacturers to foster innovation in EMC filter design

and interference mitigation. These collaborations could also explore the use of new materials and technologies to improve the efficiency of EMC filters.

6. **Adoption of Artificial Intelligence:** Investigate the use of artificial intelligence techniques to predict and dynamically adjust EMC filter parameters in real-time. This could include developing algorithms that automatically adjust filter components based on continuous monitoring of the electromagnetic environment.
7. **Publications and Dissemination:** Promote the publication of research findings and developments in international forums and specialized journals to share knowledge and best practices in the field of electromagnetic compatibility.

References

- [1] D. Chatterjee and S. K. Mazumder, “Emi mitigation of a cuk-based power-electronic system using switching-sequence-based control,” *IEEE Transactions on Power Electronics*, vol. 36, no. 9, pp. 10 627–10 644, 2021.
- [2] A. Jugoo, “Modélisation fréquentielle des convertisseurs de puissance pour l'estimation de spectres des perturbations conduites,” Somfy, Cluses, Rapport de Stage, 2023, Stage de fin d'études 5ième année d'École d'Ingénieurs.
- [3] J.-M. Redouté and M. Steyaert, *EMC of analog integrated circuits*. Springer Science & Business Media, 2009.
- [4] P. Norton, “The emc effect,” *Reports on Progress in Physics*, vol. 66, no. 8, p. 1253, 2003.
- [5] J. Ejury, “Buck converter design,” *Infineon Technologies North America (TFNA) Corn Desion Note*, vol. 1, no. 2013, 2013.
- [6] M. Veerachary, “Analysis of fourth-order dc–dc converters: A flow graph approach,” *IEEE transactions on industrial electronics*, vol. 55, no. 1, pp. 133–141, 2008.
- [7] H. Hackl, M. Stoiber, B. Auinger, T. Zengerle, F. Königseder, and J. Hansen, *Python-ltspice framework for multi-objective emc filter optimization*, IEEE, 2023.
- [8] S. Rönnberg, A. Larsson, M. Bollen, and J.-L. Schanen, “A simple model for interaction between equipment at a frequency of some tens of khz,” in *International Conference on Electricity Distribution: 06/06/2011-09/06/2011*, 2011.
- [9] F. Asadi, *Essential circuit analysis using LTspice®*. Springer Nature, 2022.
- [10] C. May, “Passive circuit analysis with ltspice,” *Springer*;, 2020.

- [11] X. Du, L. Zhou, and H.-M. Tai, “Double-frequency buck converter,” *IEEE Transactions on Industrial Electronics*, vol. 56, no. 5, pp. 1690–1698, 2009.
- [12] O. Hen, D. W. Higinbotham, G. A. Miller, E. Piaseczky, and L. B. Weinstein, “The emc effect and high momentum nucleons in nuclei,” *International Journal of Modern Physics E*, vol. 22, no. 07, p. 1330017, 2013.
- [13] T. Williams, *EMC for product designers*. Newnes, 2016.
- [14] J.-P. Roche, J. Fribe, and O. Niggemann, “Knowledge based grey box modeling of inaccessible circuits for system emc-simulation in time domain,” in *2022 24th European Conference on Power Electronics and Applications (EPE'22 ECCE Europe)*, IEEE, 2022, pp. 1–10.
- [15] J.-P. Roche, J. Fribe, and O. Niggemann, “Neural network modeling of nonlinear filters for emc simulation in discrete time domain,” in *IECON 2021–47th Annual Conference of the IEEE Industrial Electronics Society*, IEEE, 2021, pp. 1–7.
- [16] S. Kumar and D. M. Das, “Python-ltspice co-simulation to train neural networks with memristive synapses to learn logic gate operations,” in *2021 IEEE International Symposium on Smart Electronic Systems (iSES)*, IEEE, 2021, pp. 147–152.
- [17] L. Jiang, F. Wang, K. Szolusha, and K. Mathews, “A practical method for separating common-mode and differential-mode emissions in conducted emissions testing,” *Analog Devices Technical Journal*, vol. 55, no. 1, pp. 1–12, Jan. 2021. [Online]. Available: <https://www.analog.com>.

Appendix A

1. Behavior of LISN Model

A LISN (Line Impedance Stabilizer Network) is a device that allows for measurement while isolating the source from a device under test (DUT) [13]. It facilitates the direct reading of conducted disturbance voltages in both phase and neutral power supply channels. A LISN can be simulated using LTSpice software, following the structure shown in Figure 2.

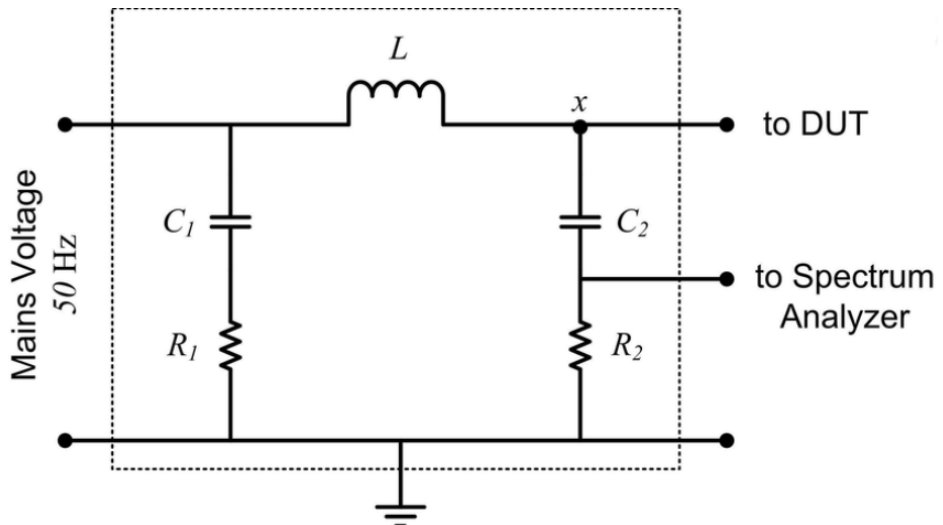


Figure A.1: Model of LISN.

Observing the frequency behavior of the LISN (Figure 3), we note that as the frequency increases, the LISN maintains an impedance of 50Ω . This means that impedance variations between the source and the DUT do not affect the disturbance voltage measurements at the LISN's terminals, because the impedance remains almost constant at 50Ω across the entire analyzed frequency band.

Therefore, as disturbance measurements are carried out in both the phase and neutral, a

LISN is incorporated for each power supply channel. Figure 4 illustrates the LISN model that will be implemented to allow the measurement of waveforms or spectra in simulation on these channels.

In Figure 4, it can be observed that the measurements from the phase (VLISN1) and neutral (VLISN2) are correctly referenced to 50Ω .

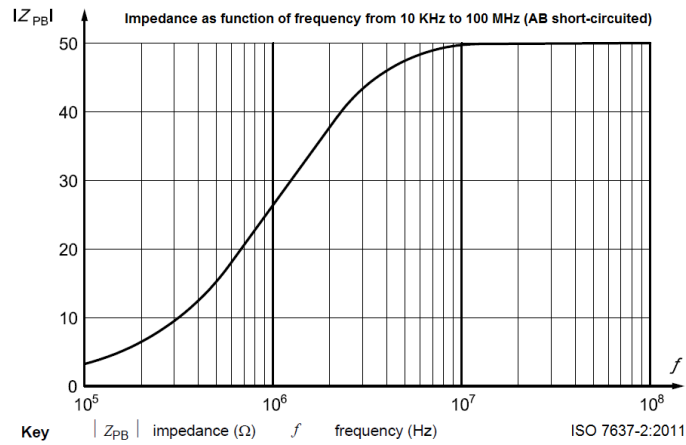


Figure A.2: Frequency behaviour of the input impedance of LISN.

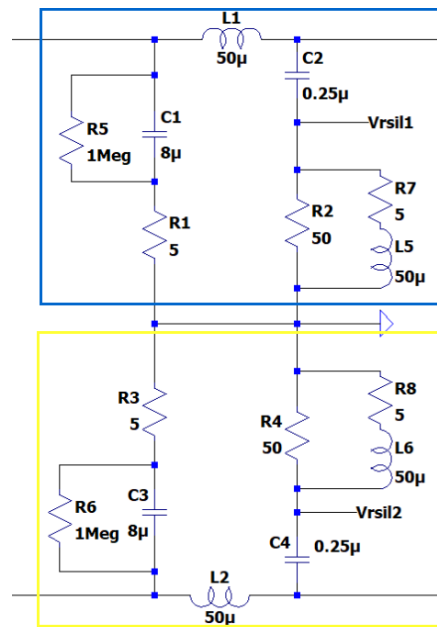


Figure A.3: Model of LISN high side (Blue), low side (yellow).

However, as mentioned before, there are two possible propagation modes: common mode and differential mode (Figure 1). The structure presented in Figure 4 does not distinguish these modes. If only one of these modes were considered, different LISN configurations would be necessary. For common mode propagation, the two 50Ω resistances would be in parallel, resulting in an impedance almost of 25Ω . In contrast, for differential mode propagation, the two 50Ω resistances would be connected in series, increasing the impedance almost to 100Ω , [2]

Appendix B

2. Explanation of Common Mode (CM)

Noise and Differential Mode (DM) Noise

Common Mode (CM) Noise

Common mode (CM) noise in conducted emissions refers to electromagnetic interference that appears between the power lines and the ground plane. This type of noise is characterized by its tendency to emit the same signal across all power lines simultaneously relative to the ground or mass, acting symmetrically and balanced.

CM is particularly problematic because it can couple through the parasitic capacitance present in the environment of electronic devices. For example, in the case of a buck converter (voltage step-down), CM noise is generated due to stray capacitance towards a ground plane, like a copper test table, through which the noise transmits or "leaks." This type of noise can be measured using power combiners in 0° configurations, which vectorially sum the input signals to obtain the magnitude of the CM noise.

Differential Mode (DM) Noise

On the other hand, differential mode (DM) noise is generated between the supply and return lines directly, without directly involving the ground plane. This noise results from voltage differences along transmission lines or circuits, manifesting as a signal that varies differentially between these lines.

In testing configurations for DM, power combiners in 180° configurations are used. These combiners vectorially subtract the input signals to determine the magnitude of the DM noise. Identifying and measuring this type of noise is critical because the techniques for mitigating CM noise are not effective for DM, and vice versa.

Common Mode and Differential Mode propagation path

The provided figure 4 illustrates a circuit used for measuring common mode (CM) and differential mode (DM) emissions in conducted emissions (CE) testing employing a buck converter. Such tests are crucial for assessing the electromagnetic compatibility (EMC) of electronic devices.

The power supply provides energy to the circuit, while a Line Impedance Stabilization Network (LISN) is utilized to filter any external noise, ensuring that only noise generated by the buck converter is measured. The LISN also serves to isolate the device under test from the power source. Two 50 Ohm resistors are included in the circuit to detect the voltages $V1$ and $V2$, which are essential for calculating the CM and DM noise components.

Common mode noise (depicted in red in the diagram) arises from potential differences between the power lines and the ground plane. This noise is characterized by being symmetric and balanced across the lines relative to the ground. On the other hand, differential mode noise (indicated in blue) occurs between the power lines, i.e., between $V1$ and $V2$. This noise results from differences in current flow through these lines and is not symmetric.

The equations shown in the diagram, $V1 = V_{CM} + V_{DM}$ and $V2 = V_{CM} - V_{DM}$, demonstrate how the measured voltages can be decomposed into their common mode and differential mode components. To calculate these components, the equations $V_{CM} = \frac{V1+V2}{2}$ and $V_{DM} = V1 - V2$ are used. V_{CM} represents the average of the voltages, reflecting the noise that is common to both lines relative to the ground. V_{DM} represents half of the difference between the voltages, indicating the differential noise between the lines.

Understanding and being able to measure and separate these two types of noise are crucial for designing effective electromagnetic interference (EMI) suppression solutions. Different mitigation techniques are effective against specific types of noise, so knowing their origins and characteristics allows for the application of the most appropriate corrective measures. This not only helps to improve the electromagnetic compatibility of the device but also ensures compliance with regulatory standards, thereby enhancing the reliability and functionality of the device in real operational environments.

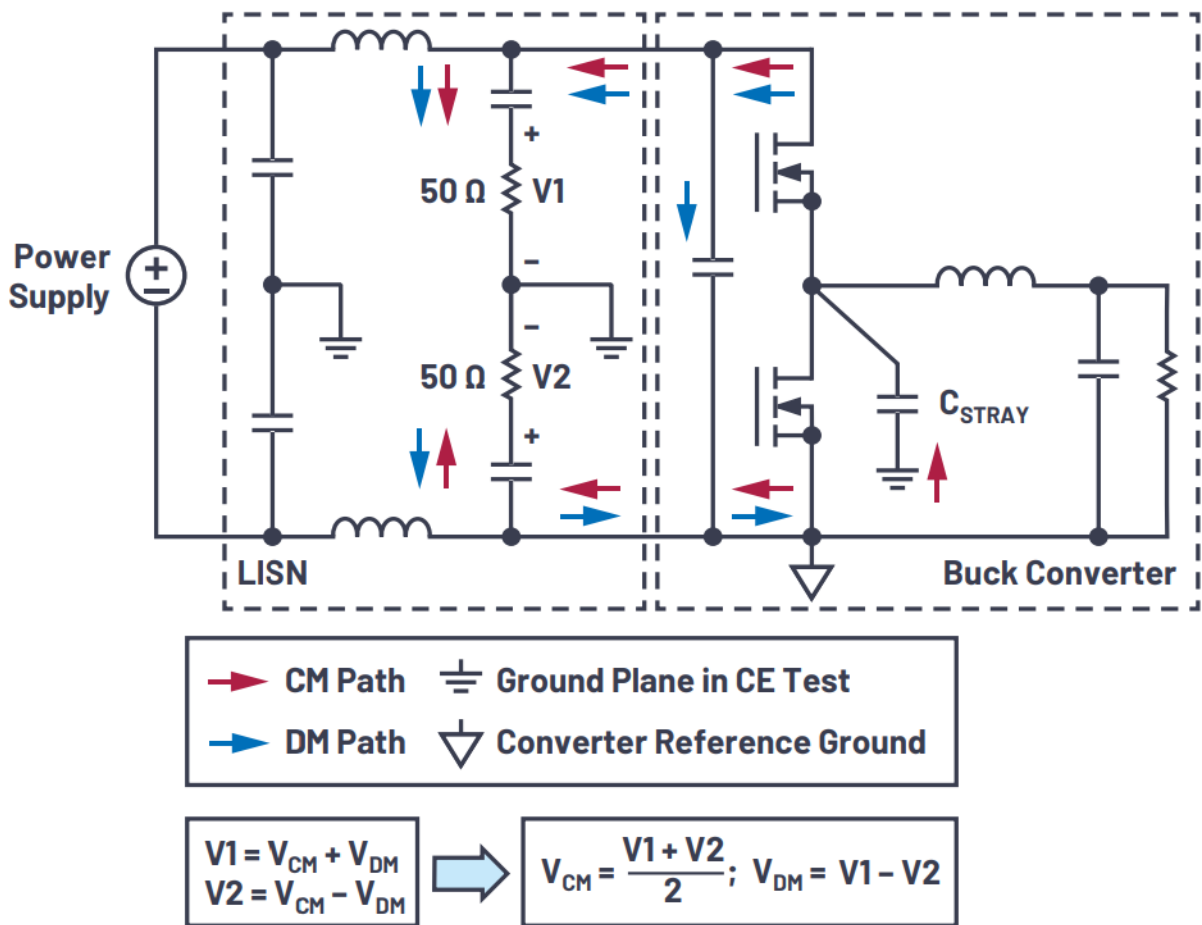


Figure B.1: Common Mode and Differential Mode propagation path [17].